

EVIDENCE OF NEOTECTONIC ACTIVITY IN SOUTHWEST LOUISIANA

A Thesis

Submitted to the Graduate Faculty of the
Louisiana State University and
Agricultural and Mechanical College
in partial fulfillment of the
requirements for the degree of
Master of Science in Engineering Science

in

The Interdepartmental Program in Engineering Science

by
Jordan Oliver Heltz
Bachelor of Science in Geology, Louisiana State University, 2000
August 2005

ACKNOWLEDGMENTS

For their emotional and financial support throughout my graduate work, I must express my appreciation and love toward my parents, Michael and Libby Heltz. Without the encouragement they provided during my college years I would not be in the position I am in today. I must also thank my sister, Ashley, and brother, Jonathan, whose success in school and life I have always tried to emulate. I must extend my gratitude to my friends for making me laugh and being there for me when I needed them most.

I sincerely thank my mentor and major advisor, Dr. Roy K. Dokka, for his guidance, patience, and support throughout my graduate studies and for providing me with the opportunity to return to school and improve my life. I also thank Dr. David Constant and Dr. Frank Tsai for being a part of my advisory committee and giving recommendations for improving this paper. My thanks also go to Mr. Kurt Shinkle and Mr. Clifford Mugnier whose technical advice was essential to the completion of this research project. Finally, I would like to extend special thanks to Blake Amacker for helping me perform the fieldwork for this study and for being a good friend on whom I could always rely.

TABLE OF CONTENTS

ACKNOWLEDGEMENTS	ii
LIST OF TABLES	v
LIST OF FIGURES	vi
ABBREVIATIONS	viii
ABSTRACT	ix
CHAPTER 1. INTRODUCTION	1
1.1 Overview	1
1.2 Goals and Objectives	3
1.3 Testable Hypotheses.....	3
1.4 Significance.....	4
1.5 Scope	5
CHAPTER 2. LITERATURE REVIEW	8
2.1 Gulf of Mexico Evolution	8
2.2 Geology of the Study Area	9
2.3 Origin and Characteristics of Gulf Coast Faults	11
2.4 Origin and Characteristics of Salt Structures	15
2.5 Related Studies of Gulf Coast Fault Activity	17
2.6 Causes of Fault Movement.....	20
CHAPTER 3. METHODS AND DATA	22
3.1 Topographic Mapping with LIDAR	22
3.2 Geodetic Leveling Data	22
3.3 Leveling Procedure	24
3.4 Equipment	27
CHAPTER 4. RESULTS	29
4.1 Areas of Interest	29
4.1.1 Indian Village Area	29
4.1.2 Iowa Area	33
4.1.3 Moss Lake Area	36
4.1.4 Vinton Area	39
4.1.5 Sulphur Area	43
4.1.6 Moss Bluff Area	47
4.1.7 DeQuincy Area	50
4.2 Calculation of Errors	50
4.3 Summary of Results	54
CHAPTER 5. DISCUSSION	55
5.1 Nature of Active Faulting	55
5.2 Causes of Recent Fault Activity in Study Area.....	56
5.3 Subsurface Fluid Withdrawal	57
5.4 Neotectonic Structural Framework	62

CHAPTER 6. CONCLUSIONS AND RECOMMENDATIONS	65
6.1 Conclusions	65
6.2 Recommendations	66
REFERENCES	67
APPENDIX A: GLOSSARY	74
APPENDIX B: SUBSIDENCE PROFILE	76
APPENDIX C: FIELD PHOTOGRAPHS	77
VITA	80

LIST OF TABLES

Table 3.1 Historical leveling lines.....	25
Table 4.1 Summary of results.....	54

LIST OF FIGURES

Fig 1.1 Map of the study area with locations of previously identified fault-line scarps.....	1
Fig 1.2 Cross-section through a typical active Gulf Coast normal fault	2
Fig 1.3 Effect of fault movement on a rigid structure built on an active fault	5
Fig 1.4 Map of Louisiana showing the limits of the study area.....	7
Fig 2.1 Tectonic map of the northwestern Gulf of Mexico	9
Fig 2.2 Control of rollover on a typical listric normal fault of the Gulf Coast.....	12
Fig 2.3 Map of the principal strike fault systems in the Gulf Coast.....	13
Fig 2.4 Map of southern Louisiana showing fault trends identified by Ocamb.....	14
Fig 2.5 Fault systems of southern Louisiana mapped by Murray.....	15
Fig 2.6 Locations of salt structures in study area and depths to the top of salt.....	16
Fig 3.1 LIDAR relief map showing the parishes and cities in the study area.....	23
Fig 3.2 Leveling technique and calculations.....	25
Fig 3.3 Leveling equipment	28
Fig 4.1 LIDAR image with fault-related steps, salt features and areas of interest.....	30
Fig 4.2 Uninterpreted LIDAR image of the Indian Village area.....	31
Fig 4.3 The Indian Village fault-related step and adjacent benchmarks	32
Fig 4.4 Uninterpreted LIDAR image of the Iowa area.....	34
Fig 4.5 The Iowa fault-related step and adjacent benchmarks.....	35
Fig 4.6 Uninterpreted LIDAR image of the Moss Lake area.....	37
Fig 4.7 The Moss Lake fault-related step and adjacent benchmarks	38
Fig 4.8 Uninterpreted LIDAR image of the Vinton area.....	40
Fig 4.9 The Vinton fault-related steps and adjacent benchmarks.....	41
Fig 4.10 Uninterpreted LIDAR image of the Sulphur area.....	44
Fig 4.11 The Sulphur fault-related step and adjacent benchmarks.....	45
Fig 4.12 Uninterpreted LIDAR image of the Moss Bluff area.....	48

Fig 4.13 The Moss Bluff fault-related step and adjacent benchmarks.....	49
Fig 4.14 Uninterpreted LIDAR image of the DeQuincy area.....	51
Fig 4.15 The DeQuincy fault-related step.....	52
Fig 5.1 Graph of average slip rates vs. groundwater withdrawal in Calcasieu Parish	57
Fig 5.2 Spatial association of groundwater withdrawal with accelerated faulting.....	58
Fig 5.3 Subsidence of benchmarks in the Lake Charles Industrial District	61
Fig 5.4 Record of water levels in well Cu-77 near Westlake.....	62
Fig 5.5 Neotectonic structural framework of the study area.....	64
Fig B.1 Relative subsidence profile through the study area.....	76
Fig C.1 Photo of the Iowa fault-related step near Iowa.....	77
Fig C.2 Photo of the Moss Lake fault-related step near Moss Lake	77
Fig C.3 Photo of the Sulphur fault-related step near Sulphur.....	78
Fig C.4 Photo of the Sulphur fault-related step near Westlake.....	78
Fig C.5 Photo of the Moss Bluff fault-related step near Moss Bluff	79
Fig C.6 Photo of the DeQuincy fault-related step near Perkins.....	79

ABBREVIATIONS

Benchmark	BM
Difference	Diff.
Digital Elevation Model.....	DEM
Gulf of Mexico	GOM
Height	Ht.
Light Detection and Ranging	LIDAR
National Geodetic Survey	NGS
Permanent Identifier	PID

ABSTRACT

A methodology that combines high-resolution topographic mapping, field observations, subsurface evaluation, and geodetic data analysis has successfully located several fault-related geomorphic steps in an area of southwestern Louisiana once thought to be relatively devoid of such features. Comparison of height differences of benchmarks straddling these suspected fault-related steps shows that vertical displacement rates on faults in the study area ranged from about 2 mm/yr to as much as 6 mm/yr during the 1960's and 1970's. However, leveling data obtained as recently as January 2005 reveals that the majority of these faults are currently moving at rates of less than 1 mm/yr.

This study identifies the presence of several previously mapped fault-related steps as well as some unidentified geomorphic features with the use of LIDAR (Light Detection and Ranging) digital elevation models and aerial photography. The majority of these topographic steps correlate well with upward projections of known subsurface faults, which suggests that they are of tectonic origin. Also, field observations have located offsets of roadways and damage to built structures due to the differential motion caused by active faulting. These lines of evidence, combined with the leveling data, suggest that the geomorphic features in the study area are the surface expressions of active faults that have moved during the past half-century. A possible cause for the accelerated fault slip rates computed for the 1960's and 1970's could be the substantial lowering of the piezometric surface that occurred due to increased subsurface fluid withdrawal. This suggests that in addition to the natural causes of faulting, anthropogenic activities may have also affected fault motion in this area of Louisiana.

CHAPTER 1 INTRODUCTION

1.1 Overview

Newly acquired LIDAR (Light Detection and Ranging) imagery in southwest Louisiana has enabled the identification of several topographic features that suggest this area may be tectonically active. Whereas some of these features have been mapped previously (Figure 1.1), most have gone undetected until recently. The recognition that other similar features in the Gulf Coast region are related to faulting suggests that the topographic steps mapped in the study area are also of tectonic origin. In this study, LIDAR imagery, aerial photography and field observations were utilized to locate and precisely map the topographic features of the area. A subsurface evaluation was performed to determine if these features are related to faulting and geodetic data were analyzed to investigate fault behavior.

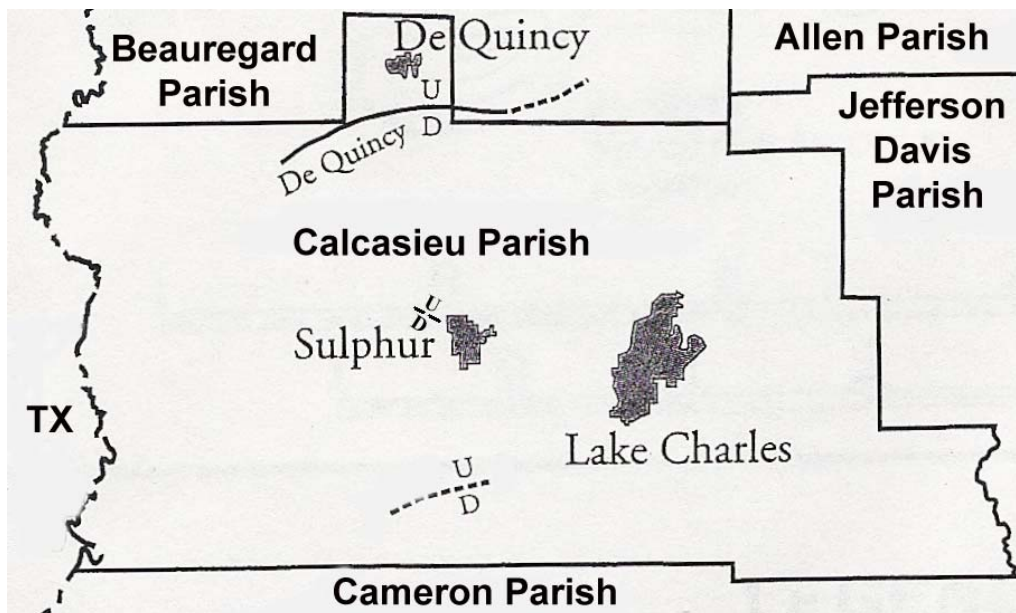


Figure 1.1. Map of the study area with locations of previously identified fault-line scarps (U = upthrown side, D = downthrown side). (modified from Heinrich, 2000 and Snead et al., 2002)

Previous studies of Gulf Coast neotectonics have referred to the surface expression of active faults in the region as “fault-line scarps” (Heinrich, 2000; Miller and Heinrich, 1998; Gagliano et al., 2003). Although this term typically implies a steeply sloping, fault-related

topographic feature, the majority of faults in the Gulf Coast region exhibit relatively gentle slopes at the ground surface. Due to this discrepancy, it is proposed that an alternate term for these geomorphic features be used, i.e., “fault-related steps”. These steps are the result of differential erosion and deposition along a fault trace and are generally imperceptible in the field at outcrop scale. Because the uppermost layers of sediment in the Gulf Coast region are poorly consolidated, fault deformation is typically in the form of cataclastic flow (Scholz, 1998). Consequently, faulting near the surface is characterized by a zone of diffuse strain, where the fault actually horsetails, rather than being marked by a distinct fault plane (Figure 1.2).

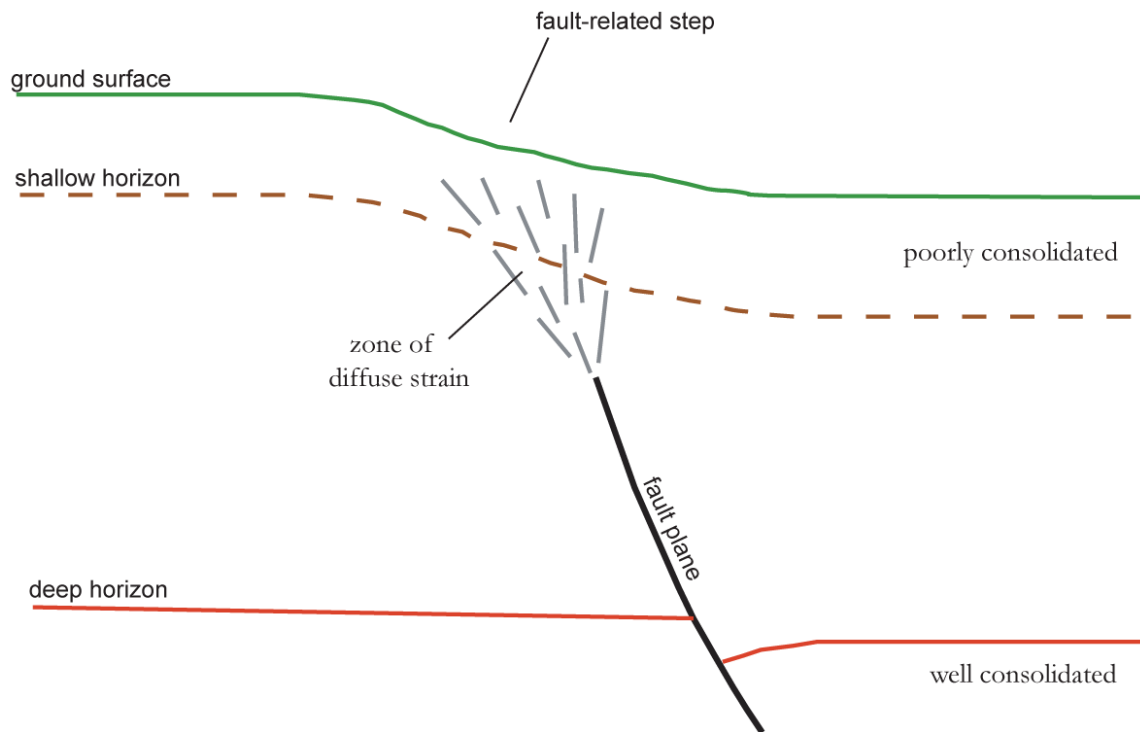


Figure 1.2. Cross-section through a typical active Gulf Coast normal fault. Image shows the nature of fault offset at the ground surface, in the shallow subsurface and at depth. Note that near the surface, these faults typically horsetail into a zone of diffuse strain rather than a distinct fault plane. (Dokka, personal communication 2005)

Field evidence of active faulting in south Louisiana is difficult to obtain due mainly to the weak nature of sediments, the subtropical climate, and the paucity of earthquakes, all of which tends to complicate their detection. Identification of faults in the region has been based on the deformation of built structures in mainly urban environments. Although observations of structural

damage are not always available, the majority of these fault-related steps exhibit a distinct topographic signature, which eases their identification on LIDAR and other imagery. Faults in other tectonically active areas such as California or the Basin and Range province are considered active when earthquakes, geomorphic landforms, or other physical signs of movement can be detected. However, these manifestations of faulting are rarely seen in the Gulf Coast and thus an alternate means of determining fault activity is required. In this study, geodetic leveling techniques were used to investigate the displacement associated with these suspected faults. Geodetic leveling has been used successfully in many areas to locate and determine activity of faults (Holzer and Gabrysch, 1987; Kebede, 2002; Gagliano et al., 2003).

1.2 Goals and Objectives

The goal of this study was to gain a better understanding of the neotectonic activity in the study area, particularly the role and origin of normal faulting. To achieve this goal required accomplishing the following objectives:

- Locate and precisely map the numerous geomorphic steps in the study area;
- Determine if these features are related to faulting;
- Investigate the nature of recent fault displacement;
- Determine the origin(s) of neotectonic activity in the study area.

Aerial photographs, field observations, and high-resolution LIDAR imagery were used to identify the topographic anomalies. In order to ascertain the origin of these features and confirm that they are fault related, an evaluation of subsurface data was performed. In addition, historical and recently acquired geodetic leveling data were analyzed to verify fault activity and quantify the nature of fault displacement.

1.3 Testable Hypotheses

This research program was designed to test the hypothesis that normal faults in the Gulf Coast region exhibit episodic motion. While it has been well established that movement on these

faults typically accelerates from the time of origin until it reaches a maximum rate and then decreases (Thorsen, 1963; Ocamb, 1961), several studies have reported varying rates of fault slip on the order of days to years (Cartwright, 1990; Reid, 1973; Holzer and Gabrysch, 1987). This study utilized geodetic data adjacent to suspected faults to examine the notion that Gulf Coast faulting occurs episodically and not continuously.

Related to possible temporal variations in fault slip is the debate over whether active faulting in the region is due to primarily tectonic or anthropogenic causes. Although most researchers agree that natural geologic forces such as lithospheric flexure, basinward sliding, and salt movement contribute to current fault activity, some have concluded that human withdrawal of subsurface fluids has recently accelerated natural fault motion (Verbeek et al., 1979; Holzer, 1984; Morton et al., 2001). To test the hypothesis that extraction of groundwater has increased natural fault motion in the study area, a temporal and spatial comparison of fluid withdrawal and fault slip rates was performed.

1.4 Significance

Determining the location and nature of movement of a geologic fault is an extremely important endeavor, not only for the benefit of academia but also for the general public. The majority of faults in the Gulf Coast region are steeply dipping normal faults that exhibit primarily down-to-the-south motion. Because of this faulting style, the displacements have vertical and horizontal components with the vertical movement often being dominant. The stresses that these displacements create on man-made structures near faults can have profound effects on the stability of those structures (Figure 1.3). Consequently, public awareness of the potential hazards to property created by fault motion is of utmost concern. However, because most faults in the Gulf Coast exhibit low relief and lack seismicity, the majority of citizens potentially affected by them are unaware of their existence. The repair of roadways, foundations, drainage projects, or other engineering works due to fault activity can become extremely expensive if the proper precautions are not taken.

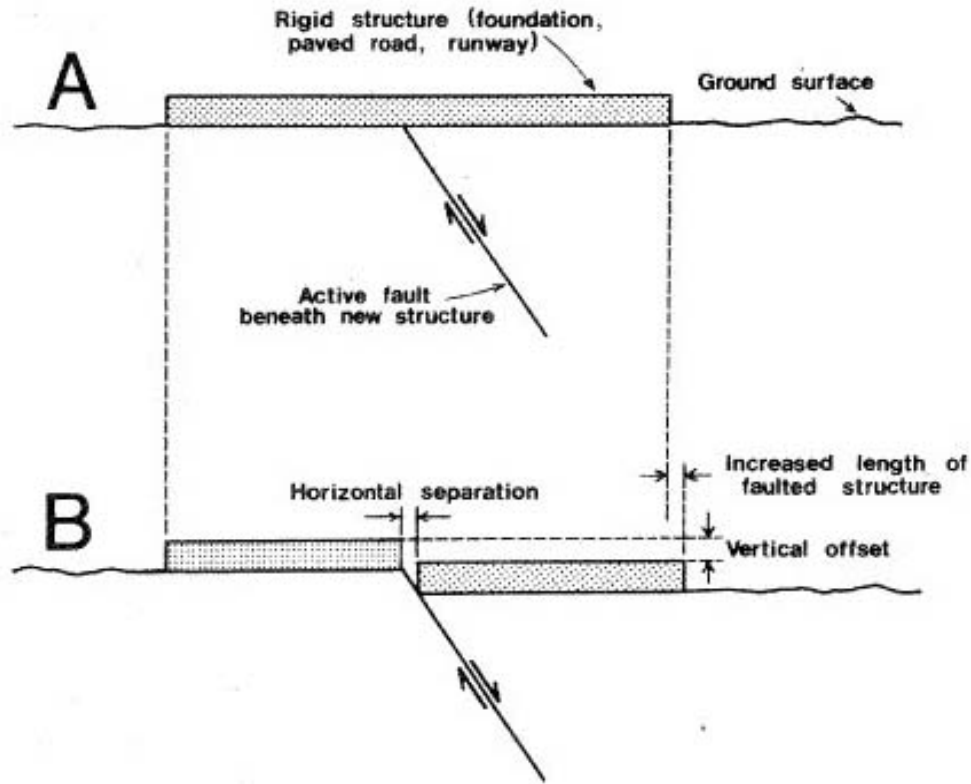


Figure 1.3. Effect of fault movement on a rigid structure built on an active fault. A, original construction; B, structure damaged by fault movement. Both vertical offset and horizontal separation are consequences of displacement. Built structures may literally be pulled apart as faulting proceeds. (Verbeek et al., 1979)

The identification of active faults in the study area and the quantification of their motions also provide new data with which to evaluate existing hypotheses regarding the nature of neotectonic activity of the northern Gulf Coast. Several of these hypotheses are the result of research done in the Houston, Texas area (Van Siclen, 1972; Kreitler, 1976; Holzer, 1984), southwestern Louisiana area (Miller and Heinrich, 2003; Heinrich, 2000), and southeastern Louisiana area (Kebede, 2002; Wintz et al., 1970; Hanor, 1982). The inclusion of this thesis in the context of these other fault studies should increase our understanding of the origins of faulting.

1.5 Scope

The study area covers over 4500 km² and encompasses all of Calcasieu Parish as well as parts of Beauregard, Allen, Jefferson Davis, and Cameron parishes (Figure 1.4). The area was

chosen because it contained a wealth of new LIDAR topographic data, geodetic data, and ancillary subsurface data. This paper provides an overview of the local geology, a discussion of the faults and salt structures in the Gulf of Mexico region, and a summary of related Gulf Coast fault studies. The topographic steps that were the focal point of this thesis are presented in a series of high-resolution LIDAR images. To confirm that the features are related to known faults required investigation of surface and subsurface data. Analysis of heights of vertical control points, called benchmarks, adjacent to these suspected faults, provides basic kinematic information about their recent motion. From this data, vertical displacements and rates of fault motion are calculated and the implications of these results are interpreted in the discussion section.

Although the methods employed in this thesis are time-tested and have been proven to be an accurate means of identifying and measuring motion along active Gulf Coast faults, there are limitations. We were unable to incorporate any shallow seismic or soil boring data into this study due to constraints on time and resources, thus subsurface evaluation of suspected faults relied solely on structural mapping by earlier researchers. Investigation of fault behavior was hampered because several benchmarks were either destroyed, could not be found, or were not visited in prior leveling projects. In addition, benchmarks were sometimes located up to a kilometer from these fault-related steps, therefore the displacements and integrated rates obtained over long distances are likely lower than the actual rates of fault movement. The reason for this is because deformation near these faults decreases with distance from the actual fault trace. Another issue that limited our ability to extensively define fault motion is that geodetic leveling strictly measures height differences, not net slip. The vertical motions measured by benchmarks are assumed to represent vertical slip rates of these suspected faults. As a result of these restrictions, only a basic investigation of fault motion could be performed. However, the observations and data presented herein do provide not only a better awareness of the active faults in the study area, but also a substantial quantitative measurement of their motion.

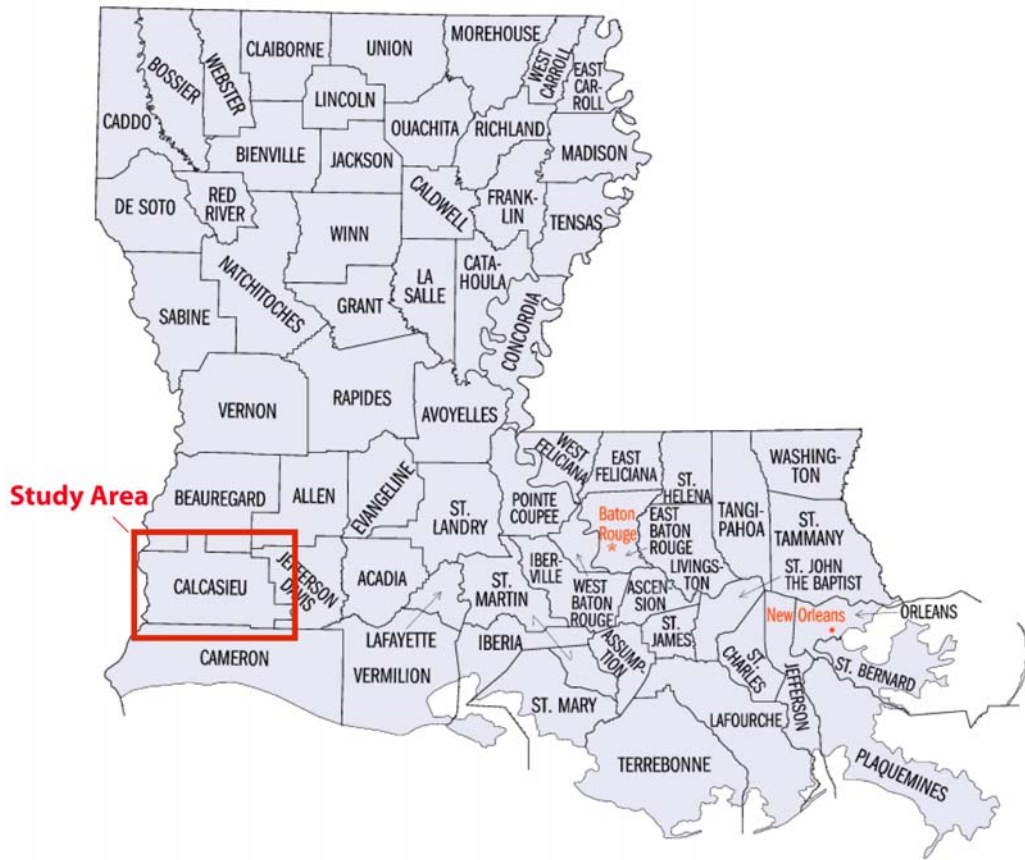


Figure 1.4. Map of Louisiana showing the limits of the study area.

CHAPTER 2 LITERATURE REVIEW

2.1 Gulf of Mexico Evolution

The Gulf of Mexico Basin originated in the Jurassic period due to thinning of the crust and sea floor spreading associated with the breakup of the supercontinent Pangea (Worrall and Snelson, 1989). It is believed that the Gulf initially opened as a result of rifting during the Middle Jurassic followed by oceanic spreading into the Late Jurassic (Peel et al., 1995). Regional subsidence and marine incursions into the Gulf Region through the Late Jurassic resulted in the widespread deposition of evaporites. These deposits, especially the Jurassic Louann salt in the Northern GOM, largely influenced the structural evolution of the region. Rather than being laid down as a uniform blanket across the Gulf Region, Salvador (1991) has shown that the salt is actually absent over most of the oceanic crust and its thickness varies where it is present. Because of the ductility and low density of this salt, the immense amount of sediments deposited above it have been deformed and resulted in this complex, highly faulted region. Diegel et al. (1995) stated that the structural styles present in the Northern gulf region are mainly a product of sediments "prograding over deforming largely allochthonous salt structures derived from an underlying autochthonous Jurassic salt". Cenozoic depositional events, sourced primarily from the Laramide orogeny, produced a cumulative thickness of over 50,000 ft of sediment in the Gulf Region (Worrall and Snelson, 1989). The Cenozoic was characterized mainly by these large influxes of terrigenous clastic sediments as well as overpressured shale sequences, which resulted from rapid deposition. In the Coastal Zone, the Mesozoic strata are buried beneath this thick wedge of Cenozoic sediments, which have prograded the shelf hundreds of kilometers seaward and generated "growth fault" systems and coastal and offshore salt diapir provinces (Ewing, 1991). The immense weight of these deposits also loads the crust, causing further subsidence of the basin. The GOM region contains structural features that, for the most part, have been created by gravity acting on an unstable substrate in a non-orogenic environment (Nelson, 1991).

2.2 Geology of the Study Area

The study area for this thesis is in southwestern Louisiana within the Gulf Coastal Plain and encompasses all of Calcasieu Parish and parts of Beauregard, Allen, Jefferson Davis and Cameron Parishes. The area lies south of the ancient Late Cretaceous Shelf Margin (Figure 2.1) and its geology is a result of the Cenozoic depositional events that prograded beyond this feature. This outbuilding of clastic sequences formed linear bands of syndepositional normal faults, termed “growth faults” (Ewing, 1991). These regional fault trends, along with salt structures, are the distinguishing feature of Gulf Coast geology. They were formed by gravitational instability at rapidly prograding shelf margins, where huge amounts of terrestrial deposits were dumped on top of undercompacted and overpressured marine clays (Winker and Edwards, 1983).

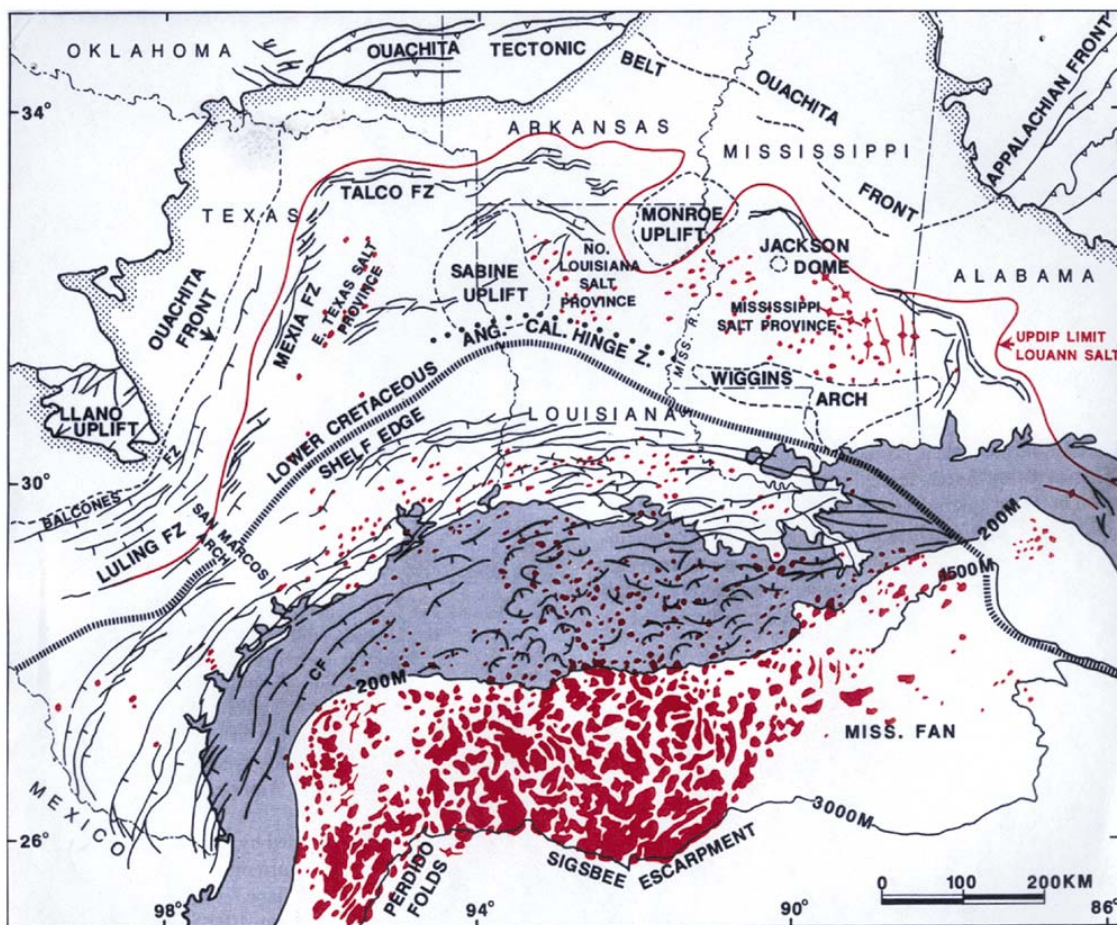


Figure 2.1. Tectonic map of the northwestern Gulf of Mexico. Salt features are shown in red. Normal faults are shown in thin black lines. Continental shelf is shown in gray. (Worrall and Snelson, 1989)

Initially prograding beyond the Late Cretaceous shelf edge was the Paleocene Midway formation, a fine-grained stable progradational shelf margin formation that lacked growth faulting. Following this was deposition of the Late Paleocene-Early Eocene Wilcox that represented an unstable delta system characterized by growth faults and submarine canyons. After deposition of the mud-dominated upper Eocene Claiborne and Jackson groups, the Vicksburg group of Lower Oligocene age was deposited and was characterized by sand and shale sequences. It was during the Oligocene that the Mississippi River drainage system became the primary supplier of sediments to the Gulf of Mexico Basin (Feng and Buffler, 1995) from source areas in the Ouachitas, Rockies, and southern Appalachians (Tabbi-Annani, 1975). The Frio Formation of Middle to Late Oligocene was deposited during a progradational event on an unstable shelf edge. During Frio time, the thickest sediment accumulation in the Gulf Region occurred in southeast Texas and southwest Louisiana. The overlying Anahuac formation of late Oligocene age is a largely fine-grained shelf margin deposit similar to the Claiborne and Jackson (Worrall and Snelson, 1989). During the substantial deposition of the Oligocene, upward movement of salt began in the central portion of the study area. This diapirism created positive features on the sea floor and influenced the sedimentation and structural development of the area as virtually all the faulting in this trend is a direct result of salt movement (Ocamb, 1961). The Miocene deposits of southwestern Louisiana were formed over unstable shelf margins with abundant growth faulting. The deltas of the ancestral Mississippi River built out the coastline of south Louisiana extensively during the Miocene. During the early part of the Miocene, the focus of deposition was near the study area of southwestern Louisiana then shifted eastward, closer to the location of the present delta (Rainwater, 1964). The overlying Foley Formation of Pliocene age includes the Evangeline aquifer, which contains mostly salt water in the study area but is heavily pumped in the areas to the north and west where it contains fresh water. Deposits of Pleistocene age cover the majority of the surface of the study area and also provide the primary source of groundwater for southwestern Louisiana, especially the Pleistocene Chicot Aquifer. The southern portion of the

study area and the alluvial valleys of the Calcasieu and Houston Rivers consist of primarily fine-grained Holocene age deposits.

2.3 Origin and Characteristics of Gulf Coast Faults

As stated previously, the majority of faults that form in the Gulf of Mexico region are termed “growth faults” where normal motion is contemporaneous with sediment deposition. This movement results in great thickening of correlative section from the upthrown block to the downthrown one (Ocamb, 1961). Most Gulf Coast faults also dip at relatively steep angles (40 to 60°) and can be described as being listric, meaning they are concave upward. The younger, more gulfward fault systems of south Louisiana tend to dip more steeply than the older landward ones (Murray, 1961). As a result of progressively increasing pore pressures below the surface (Bruce, 1973) and the increasing ductility of the rocks at depth (Shelton, 1984), the majority of growth faults tend to be steeper near the surface and become flatter with depth. In order to fill the gap created along the steeper, shallower section as the downthrown block moves away from the upthrown one, the beds on the downthrown side of these faults often dip into the fault plane, a feature known as “reverse drag” or “rollover” (Figure 2.2).

It is generally accepted that these faults owe their origin and motion to gravity instabilities associated with the accumulation of sediment loads and salt deformation in the Northern Gulf of Mexico Region. They have formed due to the extension and subsidence of the Gulf of Mexico Basin and the progradation of the shelf margin hundreds of kilometer seaward. Nelson (1991) states that, “listric-normal faults are the result of coherent, differential basinward movement of the sediments above some decollement layer”. This layer is often salt or an overpressured shale bed and specifically in the study area it is believed that the majority of the faults sole onto the Eocene Jackson shale (Spencer and Sharpe, 1996). Bruce (1973) identified several possible causes of these faults including basement tectonics, underlying salt or shale movement, slumping across regional flexures, slump at the shelf edge, differential compaction of adjacent sand and shale bodies, and crustal flexure. Worrall and Snelson (1989) concluded from

their analysis of regional seismic data that gravitational instabilities created by differential sediment loading on a mobile substratum such as shale or salt was the main cause for fault activity in the northern Gulf Coast. Because the major down-to-the-basin growth faults are a result of extension, antithetic faults also commonly form to fill the potential gap created by the tensional separation. Growth faults are the result of the extensional stresses focused at the margin of prograding continental platforms (Galloway, 1986), and therefore they often form regional fault zones that trend subparallel to the present coastline (Figure 2.3).

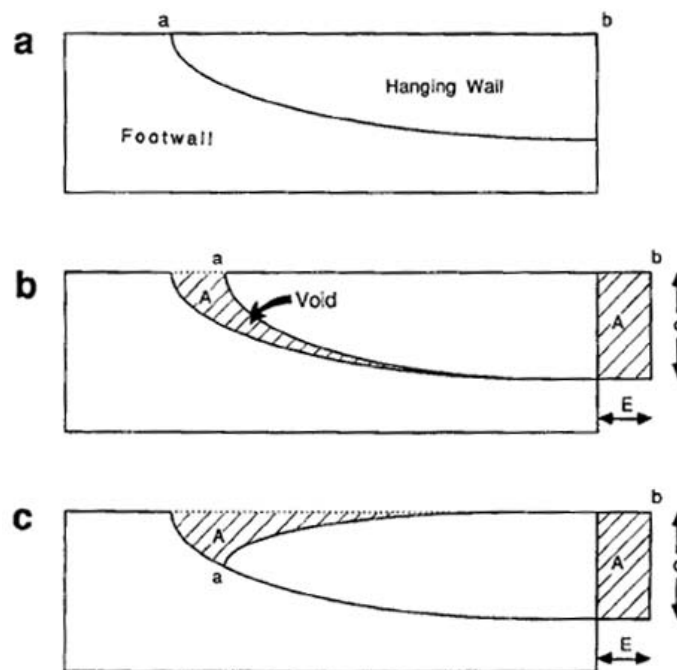


Figure 2.2. Control of rollover on a typical listric normal fault of the Gulf Coast. (Dula, 1991)

In addition to these long, linear regional fault trends, the other type of faults present in the Gulf Coast Region are those created by the movement of salt. These faults are generally short, steeply-dipping, and rather than trending in a systematic fashion, usually have various orientations. In the absence of salt diapirs, faults tend to be evenly spaced and subparallel, whereas diapir-related faults are typically sinuous or arcuate and have widely variable spacing and trends (Winker, 1982). As a natural consequence of the structural deformation of sediments by the intruding salt, all domes have associated faults (Ingram, 1991). The most common of these

terms the “Eocene Fault Trend” runs just to the north of the study area in Beauregard Parish and represents an area of faulted anticlines. At the northern border of the study area, in southern Beauregard and northern Calcasieu Parish, lies a trend of faults that are similar to the Eocene faults but are related to thickening of Oligocene Vicksburg and Jackson strata. This trend includes the prominent Baton Rouge and Tepehate fault zones and their associated fault segments, some of which exhibit surface expression in the study area. Just south of these faults lies Ocamb’s “Oligocene Domal Trend”, where the vast majority of faulting is due to salt movement and the characteristics of these faults reflects this relationship. Faulting in this domal trend is mostly of the graben or radial type, and faults are typically steeper and arcuate with widely varying orientations. During Oligocene time, this area was subsiding less than the Eocene area to the north but was relatively stable due to the presence of thick shale deposits and, according to Ocamb, this inhibited the formation of regional trend faults. Just south of this salt-dominated zone, lie regional growth fault trends of Late Oligocene to Early Miocene age (Murray’s Lake Arthur and Scott fault zones, Figure 2.5) that are characterized by relatively steep dips, linear and subparallel orientations, and significant expansion of correlative section across them.

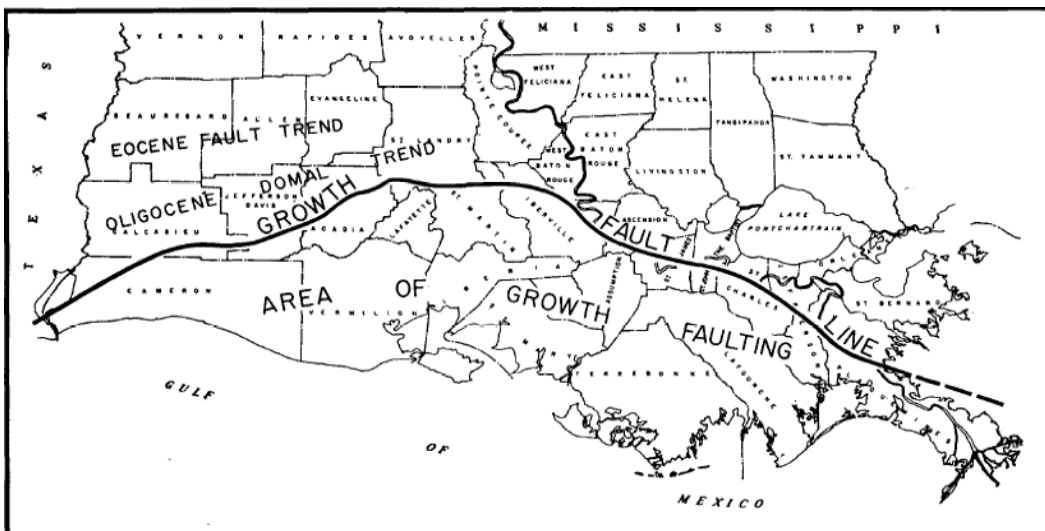


Figure 2.4. Map of southern Louisiana showing fault trends identified by Ocamb (1961).

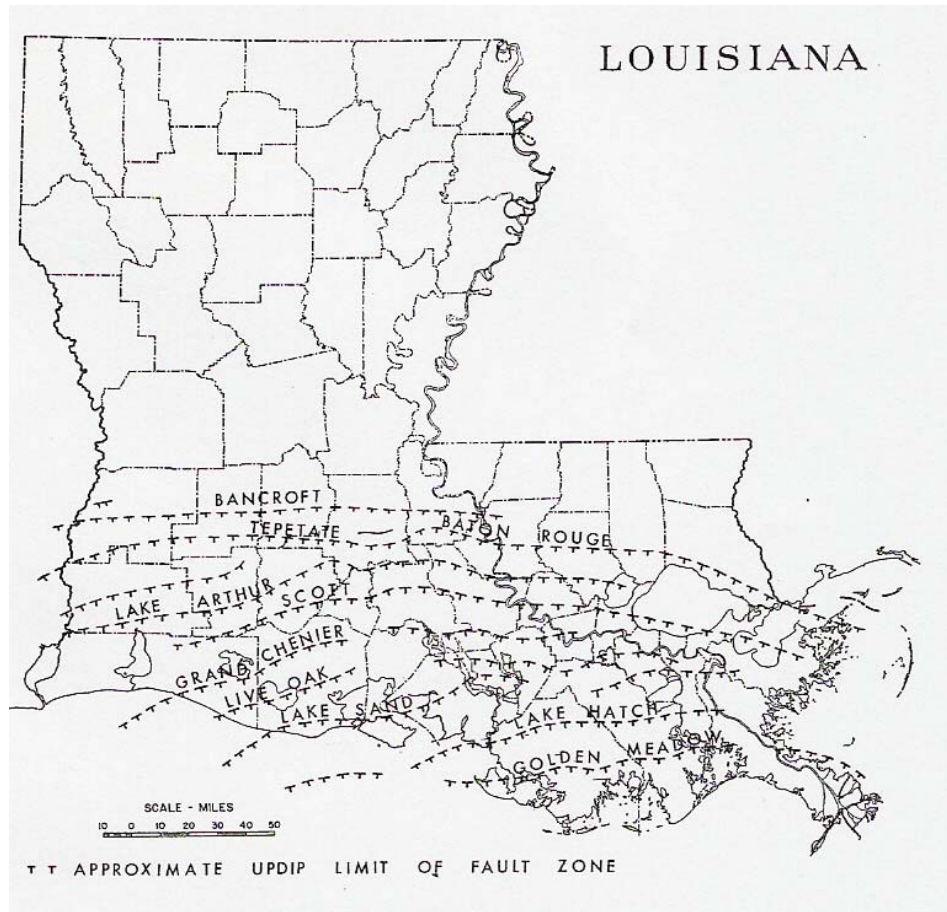


Figure 2.5. Fault systems of southern Louisiana mapped by Murray (1961).

2.4 Origin and Characteristics of Salt Structures

In the GOM region, salt flows as a result of gravitational instabilities related either to 1) surface slope, 2) differential sediment loading on top of the salt, and/or 3) buoyant forces created by more dense sediments overlying low-density salt (Nelson, 1991). The seaward progradation of thick Cenozoic sediments into the basin created salt diapirs, salt withdrawal structures, allochthonous salt features and lateral salt flow (Humphris, 1979). Loading at the updip margin of the South Louisiana salt basin by deltaic depocenters mobilized the underlying salt and this gave rise to extensive lateral salt migration and vertical salt movement (Ingram, 1991). The extent of upward growth of a salt structure is governed by buoyant forces and is therefore a function of the density of the sediments relative to the salt (Nelson, 1991). The different structural styles encountered in Gulf Coast geology are mainly a combination of the original locations of evaporite

deposits, the different slope depositional environments during the Cenozoic, and salt withdrawal from allochthonous salt sheets extruded from the Jurassic mother salt. Salt domes are frequently aligned along major growth-fault trends, and had their maximum growth after the main phase of shelf margin progradation and attendant growth faulting (Ewing, 1983). This occurrence of salt ridges and domes in association with regional fault systems suggests that the salt structures may have been positioned at depth due to 1) weaknesses in the overburden created by faulting and/or 2) increases in sedimentary thickness that occur across the fault zones (Murray, 1961). Salt structures in the GOM region are not simply post-depositional late piercing features that have risen up from the Jurassic Louann salt, but are “actually preserved remnants of large, thick, allochthonous salt masses” (Worrall and Snelson 1989). In other words, salt has not played a passive, intrusive role in the tectonics of south Louisiana but is in fact the primary control of structure in the region.

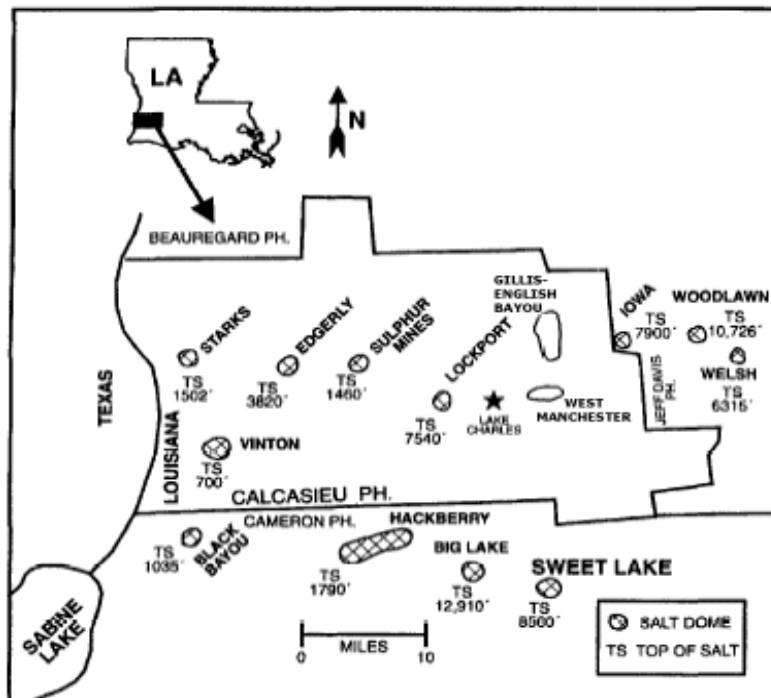


Figure 2.6. Locations of salt structures in study area and depths to the top of salt. (Spencer and Sharpe, 1993)

Several salt structures exist in the study area and are part of the South Louisiana Coastal Salt Basin. The most striking arrangement of salt diapirs in the study area is the east-west trend of

structures from Starks dome in the west to the Welsh salt dome in the eastern part of the study area (Figure 2.6). This alignment of domes probably reflects an original Jurassic/Cretaceous autochthonous salt ridge that through time with continued subsidence, burial, and downbuilding has evolved into the present day salt dome distribution (Spencer and Sharpe, 1993). The majority of the salt structures in the study area lie in what Ocamb called the “Oligocene domal trend”, a zone of salt domes that initially began upward movement in the late Eocene but saw their maximum growth during Oligocene sedimentation. Regional trend faults are rare in this area as most of the faulting results from the primary effect of salt movement (Ocamb, 1961). Because of this mode of formation, radial and graben faults dominate in this portion of the study area.

2.5 Related Studies of Gulf Coast Fault Activity

Numerous studies have been conducted regarding recent fault activity in the Gulf Coast region, especially in the Houston, TX, Baton Rouge, LA, and New Orleans, LA areas. Since very little prior work has been done concerning the existence or motions of faults in the thesis area, a review of this related research would be beneficial. One such study by Lopez et al. (1997), provided evidence for surface expression and recent movement along faults in Lake Ponchartrain, just north of New Orleans, LA, by analyzing shallow high-resolution seismic imagery and roadway offsets. These faults represent the eastward extension of the Tepehate-Baton Rouge fault system, which runs east to west across the state. They presented evidence for sustained fault movement from the Pleistocene to Recent time and calculated slip rates ranging from 2.5 to 10 mm/yr for these faults. The report concluded that these values represent “modern” rates of fault motion, which were far in excess of longer-term “geologic” rates. Gagliano et al. (2003) studied geomorphic features in Southeastern Louisiana to identify the surface expression of faults and quantify the coastal land loss that results from their movement. They correlated proven and suspected surface “scarps” with known subsurface faults and related these to the neotectonic framework of the area. Geosynclinal downwarping, sediment loading, compaction, salt movement and gravity slumping were given as causes for recent fault activity in their report.

Knowledge of active movement along the Baton Rouge fault has been suspected for several years and has been studied extensively by several researchers (Wintz et al., 1970; McCulloh and Autin, 1991; Kebede, 2002). The ongoing deformation associated with the differential movement along the Baton Rouge fault has caused noticeable damages to built structures located near the fault trace. The active motion of the Baton Rouge fault, estimated to range from 1 mm (Kebede, 2002) to 6 mm year (Wintz et al., 1970), has created a series of easily mapped fault-related steps (McCulloh and Autin, 1991; Cazes, 2004). Using a leveling technique similar to that employed in this thesis, Kebede (2002) observed that the vertical slip along the Baton Rouge fault varied considerably along strike from 1 mm/yr to 5 mm/yr during the past decade. Another study that investigated active motion along the Tepehate-Baton Rouge fault zone was conducted by Hanor (1982). He analyzed electric logs from numerous wells around the Torbert area in south-central Louisiana and constructed detailed subsurface maps in the vicinity of the Tepehate fault. This mapping led him to conclude that the Torbert segment of the Tepehate fault zone had experienced two separate periods of movement, one, which ended in the Oligocene and a second, which began in the Pleistocene and apparently, is continuing. Miller and Heinrich (2003) also studied a fault segment of the Tepehate fault zone in southwestern Louisiana that is known to extend to the ground surface and has been active in recent times. They reported that the China segment of the Tepehate fault zone exhibits surface expression consisting of a series of linear topographic features. In this study, they found evidence of “scarps” that range from 1.5 to over 3 meters in height and offset Pleistocene terraces and Holocene flood plains indicating recent movement. Perhaps the only study that investigated a fault-related topographic feature within the thesis area was conducted by Heinrich (2000) regarding the “DeQuincy Scarp”. This feature, which is also a part of the Tepehate fault zone, runs roughly east-west through the study area for over 40 km and measures up to 8 m in height. In Heinrich’s study, he evaluated fault cuts on shallow electric logs and projected this fault plane up to the surface where it clearly intersected the base of the “DeQuincy Scarp”. He also found that this fault exhibited initial movement during

Late Eocene to Oligocene time, followed by a long period of dormancy up until Plio-Pleistocene time when the fault was reactivated.

Another Gulf Coast locality with active faults is the Houston-Galveston area of Texas, where more than 160 faults totaling over 500 km in length have been identified at the land surface (Holzer, 1984). The fault issue in the Houston-Galveston area bears a remarkable resemblance to that of the study area; the two locales share a similar geology and both have experienced substantial subsurface fluid (oil, gas, and groundwater) withdrawals that may be accelerating fault motion. It also appears that the recent surface faulting around Houston, like the thesis area, is occurring along preexisting faults. Shallow seismic and borehole data have verified connections between some of the Houston area fault-related steps and growth faults in the shallow subsurface (Verbeek, 1979). These faults move by aseismic creep at rates up to 27 mm/yr (Holzer, 1984) and produce surface offset ranging in height from about 0.2 to 1.5 m (Verbeek et al., 1979). Hundreds of residential, commercial, and industrial structures in the Houston metropolitan area have sustained moderate to severe damage as a result of their locations on or near active faults. There has been a great deal of debate about whether the faults in the Houston-Galveston area owe their activity to natural geologic processes (salt movement, flexure, tilting) or to man-induced processes (withdrawal of oil, gas and groundwater). The evidence to support the former includes: 1) rising salt domes that have deformed Pleistocene sediments (Holzer, 1984), 2) a surface neotectonic framework that corresponds with that of the subsurface (Van Siclen, 1972), 3) basinward tilting of sediments indicating geologically youthful deformation (Holzer, 1984), 4) correlation of geomorphic features with preexisting faults (Verbeek et al., 1979), 5) the presence of some fault-related steps that predated any significant fluid withdrawal (Clanton and Verbeek, 1979). Evidence that suggests the latter is the case consists of: 1) seasonally variable fault creep that coincides with periods of increased groundwater withdrawal (Reid, 1973; Kreitler, 1976), 2) a spatial and temporal association between high rates of groundwater withdrawal near the Houston Ship Channel and increased fault activity (O'Neill and Van Siclen, 1984), 3) extreme

cases of hydrocarbon production that resulted in surface faulting (Holzer, 1984), 4) reductions in fault creep that coincided with reductions in rates of groundwater pumping (Holzer and Gabrysch, 1987), and 5) increase in the rates of surface offset within the last 50 years (Verbeek et al, 1979). In light of this evidence, several workers have come to the conclusion that the surface faulting in the Houston-Galveston area is the result of natural activation of Tertiary subsurface faults combined with man-induced activation from extensive subsurface fluid withdrawal in recent times (Kreitler, 1976; Holzer, 1984; Reid, 1973; O'Neill and Van Siclen, 1984).

2.6 Causes of Fault Movement

Varying theories for the causes of fault motion along Gulf Coast faults have resulted from the extensive research performed in the area. Although the faults of the Gulf Coast clearly show a basinward migration of activity with time (Thorsen, 1963) and are expected to be most active near the shelf edge (Winker, 1982), some of the older landward fault systems are still active today or show evidence of recent reactivation. According to Nunn (1985), the recent movements along these faults that were originally formed in the Eocene and Oligocene cannot be easily explained by mechanisms such as gravitational readjustment within the sedimentary section or differential compaction due to lateral density variations since those processes should decrease with time. He proposed that lithospheric flexure due to the immense sediment loading since the Pleistocene is primarily responsible for the renewed movement along some of the older regional fault systems in the Gulf Coast. The basinward downwarping and deformation of coastal sediments caused by this depression of the crust has been recognized in studies of precise geodetic leveling throughout the region (Shinkle and Dokka, 2004; Jurkowski et al., 1984). This flexure has created an extensional state of stress in the Northern Gulf of Mexico and is apparently partly responsible for the reactivation of some of the older normal faults in the region. Other researchers have felt that Gulf Coast faults owe their current activity to the continued basinward sliding of the sedimentary section due to its deposition on a sloping mobile substrate of shale and/or salt (Nelson, 1991; Worrall and Snelson, 1989). In his work with clay models, Cloos (1968) presented the idea that

the fault patterns of the Gulf Coast can be caused by “regional gravity creep of the sedimentary blanket into the basin”. In addition, the ongoing vertical movement of salt structures in the Gulf Coast Region may be locally generating fault motion as salt is being withdrawn from some areas and intruding into others creating tensional forces on the sediments. Lateral variations in lithology can result in differential compaction and consequently create shear failures and induce faulting (Bruce, 1973).

Faulting due to differential compaction is also believed to result from depressuring of reservoirs and the attendant increases in effective stress caused by these fluid pressure reductions. This type of human-induced faulting is suspected to result from the subsurface withdrawal of groundwater (Holzer, 1984; Kreitler, 1976) and hydrocarbons (Morton et al., 2001; Yerkes and Castle, 1976). However, several studies (Martin and Serdengecti, 1984; Geertsma, 1973; Holzer and Bluntzer, 1984) have discounted hydrocarbon withdrawal as a major cause of historical faulting in the Gulf Coast due to the extreme reservoir conditions which are required to produce differential compaction at the surface. O’Neill and Van Sicle (1984) proposed another mechanism by which Gulf Coast faults may be reactivated or accelerated due to lowering of the piezometric (fluid pressure) groundwater surface. They describe a process, independent of differential compaction, by which rates of natural geologic fault motion are increased due to changes in the effective stress field caused by groundwater withdrawal. Van Sicle (1972) presented the idea that increases in vertical effective stress due to groundwater withdrawal compel a “corresponding (but smaller) increase in the difference between the greatest and least principal stress, sometimes to the point where this stress difference is sufficient to cause movement along some of the pre-existing faults”.

CHAPTER 3 METHODS AND DATA

3.1 Topographic Mapping with LIDAR

In this thesis, LIDAR data was utilized to assist in the recognition and mapping of topographic features that resemble fault-related steps in southwestern Louisiana. LIDAR is an acronym that stands for Light Detection and Ranging, a remote sensing technique that uses a laser light source to determine the position, velocity, and other characteristics of distant objects. Laser altimetry is the process of using LIDAR technology to create digital elevation models, commonly referred to as DEMs. These LIDAR DEMs can be downloaded from <http://www.atlas.lsu.edu>, a website maintained by Louisiana State University.

Subtle changes in the topography of the study area are easily identified with the use of these high-resolution data sets (Figure 3.1). Topographic mapping with LIDAR DEMs can aid in the identification of previously unmapped fault-related steps in addition to better defining the locations of known features. These steps produce a topographic signature similar to that exhibited by other known fault-related geomorphic features. Preliminary evidence that suggests these features are fault-related steps includes: 1) the steps control drainage patterns, 2) they truncate older features such as alluvial ridges, 3) their morphology resembles other known fault-related steps in the area, and 4) they are associated with geologic features such as salt domes. However, remote sensing evidence alone cannot confirm that these features are in fact of tectonic origin. In this study, we utilized historical and newly acquired leveling data, subsurface structure maps, and field observations in conjunction with this LIDAR mapping to not only identify these faults but also to quantify their recent activity.

3.2 Geodetic Leveling Data

In order to investigate how suspected faults have moved over time, the change in height of locations on either side of the faults needed to be determined. Vertical control points, called benchmarks, on opposite sides of these fault-related steps have been leveled to throughout the last

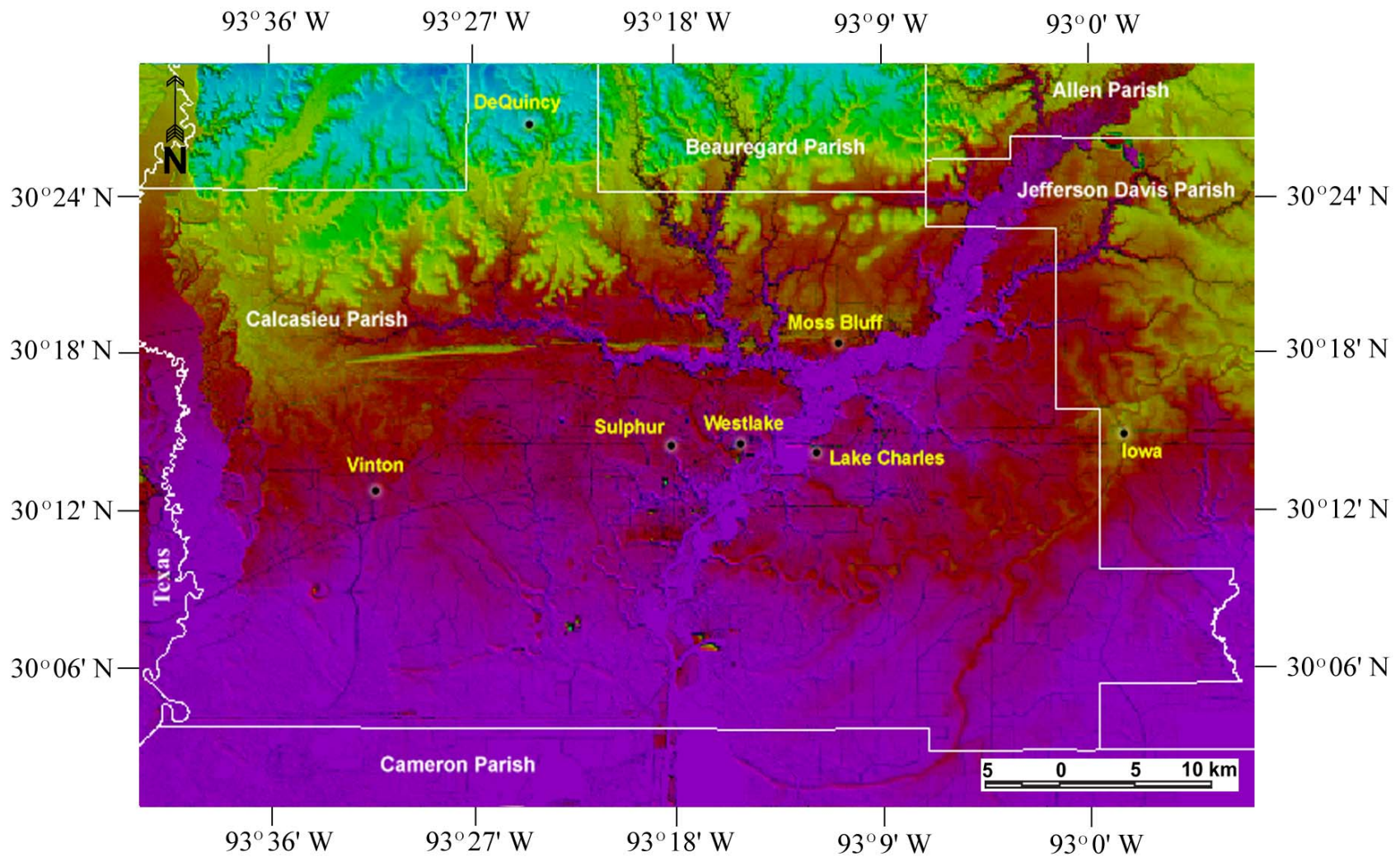


Figure 3.1. LIDAR relief map showing the parishes and cities in the study area. Darker colors (purple and red) represent low elevations; Lighter colors (green and yellow) represent higher elevations.

half-century and consequently their historical height differences have been recorded. By comparing the past height differences of benchmarks that straddle these faults, we were able to quantify the nature of recent vertical fault slip. The height differences used in this study were obtained from “phase 1” (p-files) files for 1st and 2nd order leveling lines extracted from the National Geodetic Survey’s Integrated Data Base (Table 3.1). For each leveling line, the p-file contains general information about the leveling run and data about each benchmark. The benchmark information is an ordered list of: stations (PID and BM designation), stability rating, spur level, distance along the level line, unadjusted height (elevation), number of runs, and an approximate position. The “unadjusted heights” are derived from the very precise elevation differences observed in the leveling survey process. Corrections for systematic errors (i.e. orthometric, rod, level, temp, astronomic, refraction, magnetic) were applied automatically to the observations when the p-file was generated (Shinkle and Dokka, 2004).

3.3 Leveling Procedure

In addition to the historical rates of fault slip that were computed from old leveling projects, current fault motions could also be obtained by performing new leveling transects across these faults. This was carried out by means of geodetic leveling with a Trimble DINI 12T digital level and 2-meter Invar barcode rods. Geodetic leveling is the most precise and reliable way to determine the height difference between two points (Anderson and Mikhail, 1998) and therefore it was ideal for this thesis project. Geodetic leveling is a measurement system comprised of height differences observed between nearby survey rods (Figure 3.2). With a digital leveling system, height differences are determined using near fully automatic instruments and methods. This is accomplished by a pattern recognition imaging system built into the digital level and level rods graduated with a special bar code. Using these instruments, and following NGS guidelines for 1st order/class II geodetic leveling, we measured the height differences between benchmarks on opposite sides of these fault-related steps. A benchmark is a point of known elevation and location that serves as a reference for leveling projects. In some localities the heights of these

benchmarks may change due to movements of the earth such as those caused by earthquakes, faulting, or subsurface fluid withdrawal (Anderson and Mikhail, 1998).

Table 3.1 Historical leveling lines

Location	Date of Leveling Line - (Class/Order)	Date of Leveling Line - (Class/Order)	Date of Leveling Line - (Class/Order)	Date of Leveling Line - (Class/Order)
Indian Village	1969 - (2/0)	1986 - (1/2)		
Iowa	1955 - (1/2)	1969 - (2/0)	1970 - (1/1)	1986 - (1/2)
Moss Lake	1965 - (1/2)	1982 - (1/2)		
Vinton - S	1970 - (2/0)	1981 - (1/2)		
Vinton - N	1955 - (1/2)	1972 - (1/1)	1981 - (1/2)	1986 - (1/2)
Sulphur	1965 - (1/2)	1972 - (1/1)	1982 - (1/2)	
Moss Bluff	1969 - (2/0)	1986 - (1/2)		

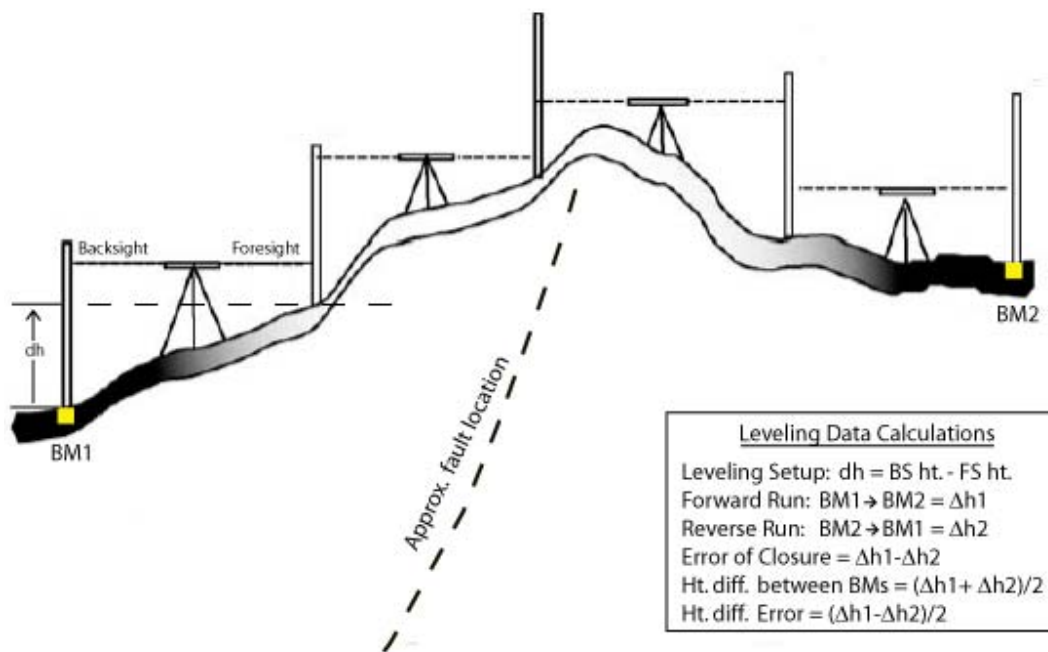


Figure 3.2. Leveling technique and calculations. (modified from Schomaker and Berry, 1981)

Leveling from one benchmark to another to determine the height difference between them requires a continuous series of leveling stations that consist of a backsight rod, the leveling instrument, and a foresight rod. By focusing the instrument on each leveling rod, heights of the respective rods can be determined with the difference between them being the change in height for that station. The foresight rod for one station then becomes the backsight rod of the next

station and this procedure is repeated until the next benchmark is reached. After one leveling run is completed, the height change from the original benchmark is computed from the difference of the sum of the backsights and the sum of the foresights. This procedure is then repeated in the opposite direction until the original benchmark is reached thus completing the level circuit. The disparity between the two height differences obtained from each run is termed the “error of closure” for that circuit. The corrected height difference between the two benchmarks is then given as the average of height differences obtained from the two level runs. Averaging the results of two runs made in opposite directions nearly eliminates any systematic accumulation of error resulting from consistent movement of the turning points (Schomaker and Berry, 1981).

Leveling lines are classified according to how well they limit the sources of known error and also to the degree of closure obtained with respect to the length of the line. In performing the fieldwork for this study, we followed the guidelines provided by the NGS Manual for 1st order / class II leveling (Bossler, 1984). The tolerances for 1st order/class II leveling are a maximum sighting distance of 60 m, a maximum imbalance in the rods of 5 m per setup and 10 m per section, and a collimation error of less than 0.05 mm/m. The maximum closure allowed for 1st order/class II leveling when surveying the same section in opposite directions is $4 \text{ mm} * \sqrt{\mathbf{K}}$, where \mathbf{K} is equal to the distance in kilometers between benchmarks. Collimation checks were performed each day in order to properly adjust the instrument to the standard of accuracy required for 1st order/ class II leveling. These checks correct the line of sight of the instrument according to the environmental conditions and apply this correction to the readings obtained by the digital level. The method we employed for making the collimation check is known as the Kukkamaki method and is widely used for this purpose. The spirit levels of the rods were also regularly calibrated to insure that the rods were correctly plumbed and would therefore provide the most accurate heights possible. Interpretation of this data required several assumptions to be made:

- 1) It was assumed that any differential movement of benchmarks located adjacent to a fault-related step was directly related to movement of the fault.

- 2) Fault motion was determined by calculating changes in relative benchmark heights over time. Slip rates were calculated by dividing the relative height changes by the amount of time between leveling runs. Therefore, these rates represent linear displacement of the fault during that time span.
- 3) Benchmarks located further away from fault-related steps may experience lower displacements than those closer to the faults since deformation typically decreases with distance from the fault trace.
- 4) Benchmark type has little effect on the magnitude of relative displacements.

3.4 Equipment

- **Leveling Instrument**

The leveling instrument used in this study was a Trimble DINI 12T Digital Level with a precision of 0.3 mm/km when using electronic measurement on Invar level rods.

- **Turning Plate**

A turning plate, or turtle as it is sometimes called, is a solid base onto which the leveling rods are placed during measurements. These plates maintain the same height for the level rods as they are “turned” between the foresight point for one station to the backsight point of the following station.

- **Tripod**

In the leveling performed for this study, a wooden tripod with three fixed legs was used, as recommended by the NGS (Bossler, 1984).

- **Leveling Rods**

Two 2-meter Invar barcode level rods were used to provide heights above turning points and benchmarks. Invar rods are made of a steel-nickel alloy that has a very small coefficient of thermal expansion. The barcode strip on these rods allows the digital leveling instrument to automatically read the distance and heights of the leveling rods.



Figure 3.3 Leveling equipment.

CHAPTER 4 RESULTS

4.1 Areas of Interest

In the following section, several areas of interest within southwestern Louisiana are investigated in detail (Figure 4.1). High-resolution LIDAR images of each area are presented as well as a summary of the subsurface evaluation and field observations for the fault-related steps in those localities. Also included in this chapter are the geodetic data that were used to compute vertical displacements and rates of fault motion.

4.1.1 Indian Village Area

The 0.5 to 1.5 m high topographic step visible in Figure 4.2 is coextensive with the projected trace of a subsurface fault (Bellamy, 1970; Paine, 1968) that has been mapped from wellbore data by several workers (Wallace, 1966; Hickey and Sabate, 1972; Bebout and Gutierrez, 1983). It is a down-to-the-south fault that is associated with hydrocarbon accumulations at the Topsy, Thompson Bluff and Indian Village Fields. Paine (1962) observed fault displacement of fluvial sediments of the Prairie Allogroup in the Wolfe Gravel Pits (lake-like features seen on the eastern portion of Figure 4.2) that likely corresponds with the mapped fault-related step. Miller and Heinrich (2003) noted that this surface faulting showed excellent correlation with a fault cut in an oil well located 1220 m south of the gravel pit exposure.

The heights determined in 1969 from leveling to benchmarks BK0860 and BK1695 were 10.90522 m and 7.91928 m, respectively, giving a height difference of 2.98594 m between these benchmarks. By comparison, the height difference between these same two benchmarks was found to be 3.04172 m in 1986. These values show that benchmark BK1695 moved down 0.06118 m relative to benchmark BK0860 over that seventeen-year period, which corresponds to a 3.6 mm/yr vertical slip rate for this fault. Because neither of these benchmarks could be recovered, it was impossible to perform additional leveling across this fault segment.

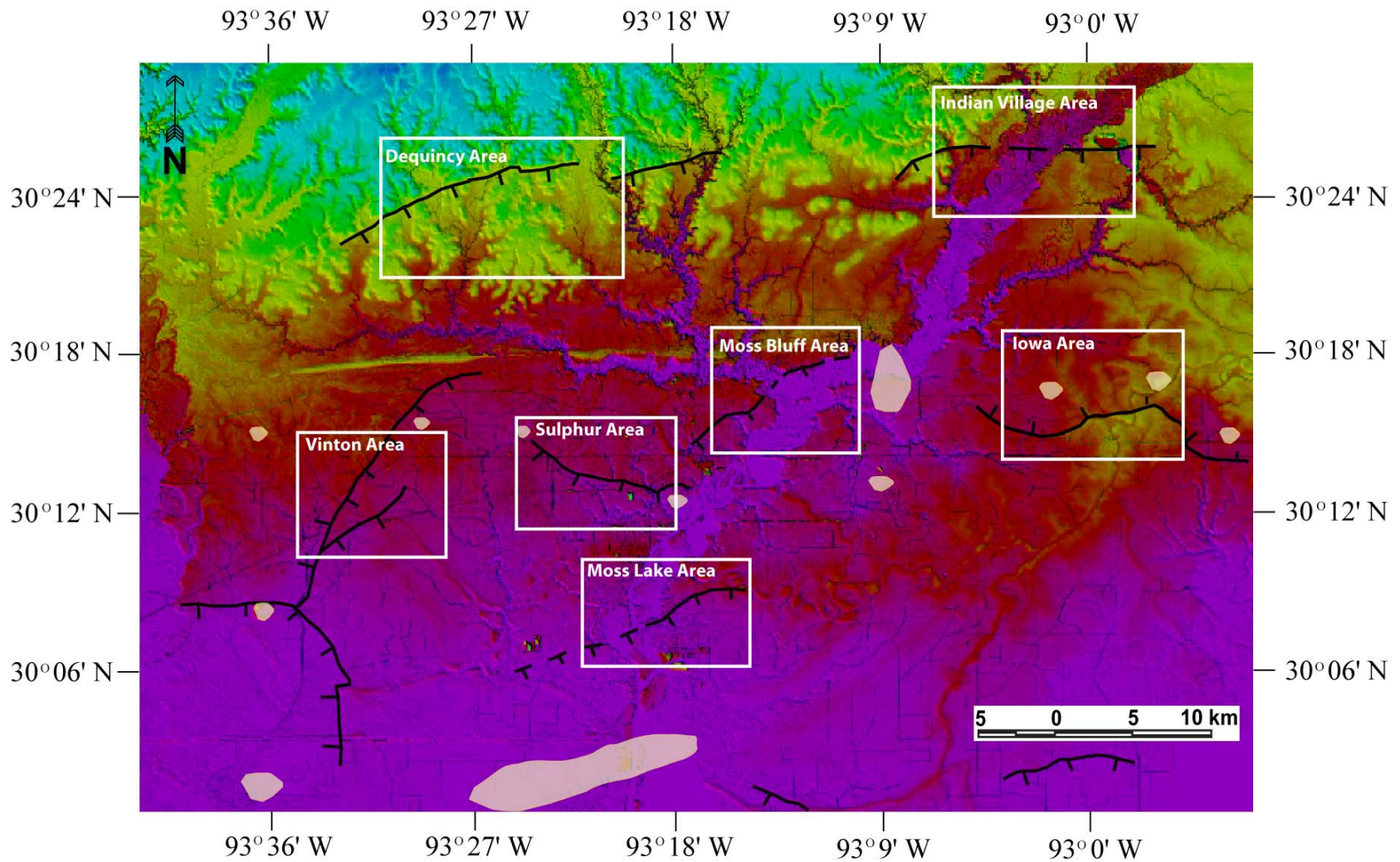


Figure 4.1. LIDAR image with fault-related steps, salt features and areas of interest. Fault-related steps are represented by black lines (teeth on downthrown side). White circles and polygons represent subsurface salt structures. Boxes are areas of interest that are investigated in detail.

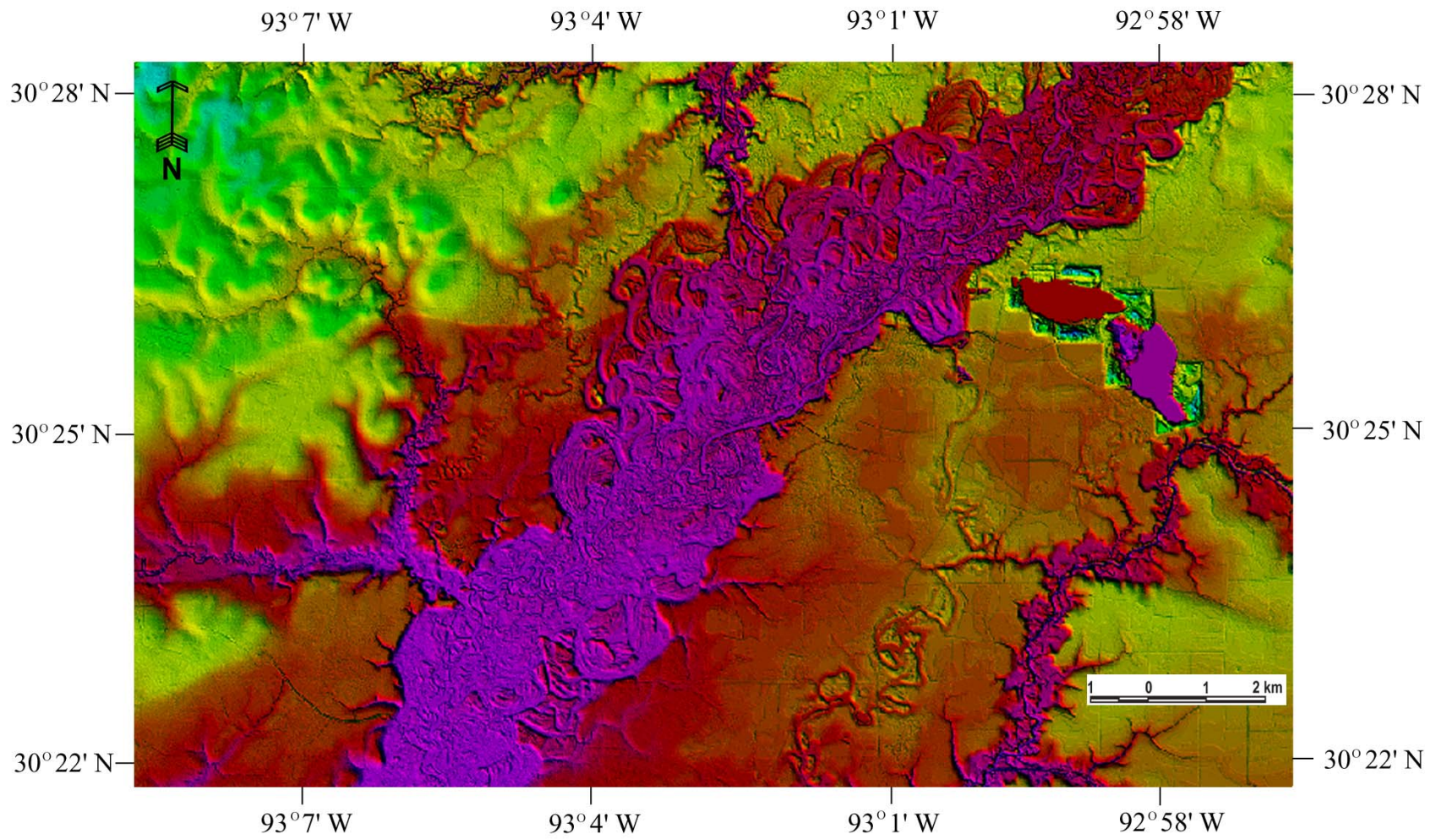


Figure 4.2. Uninterpreted LIDAR image of the Indian Village area.

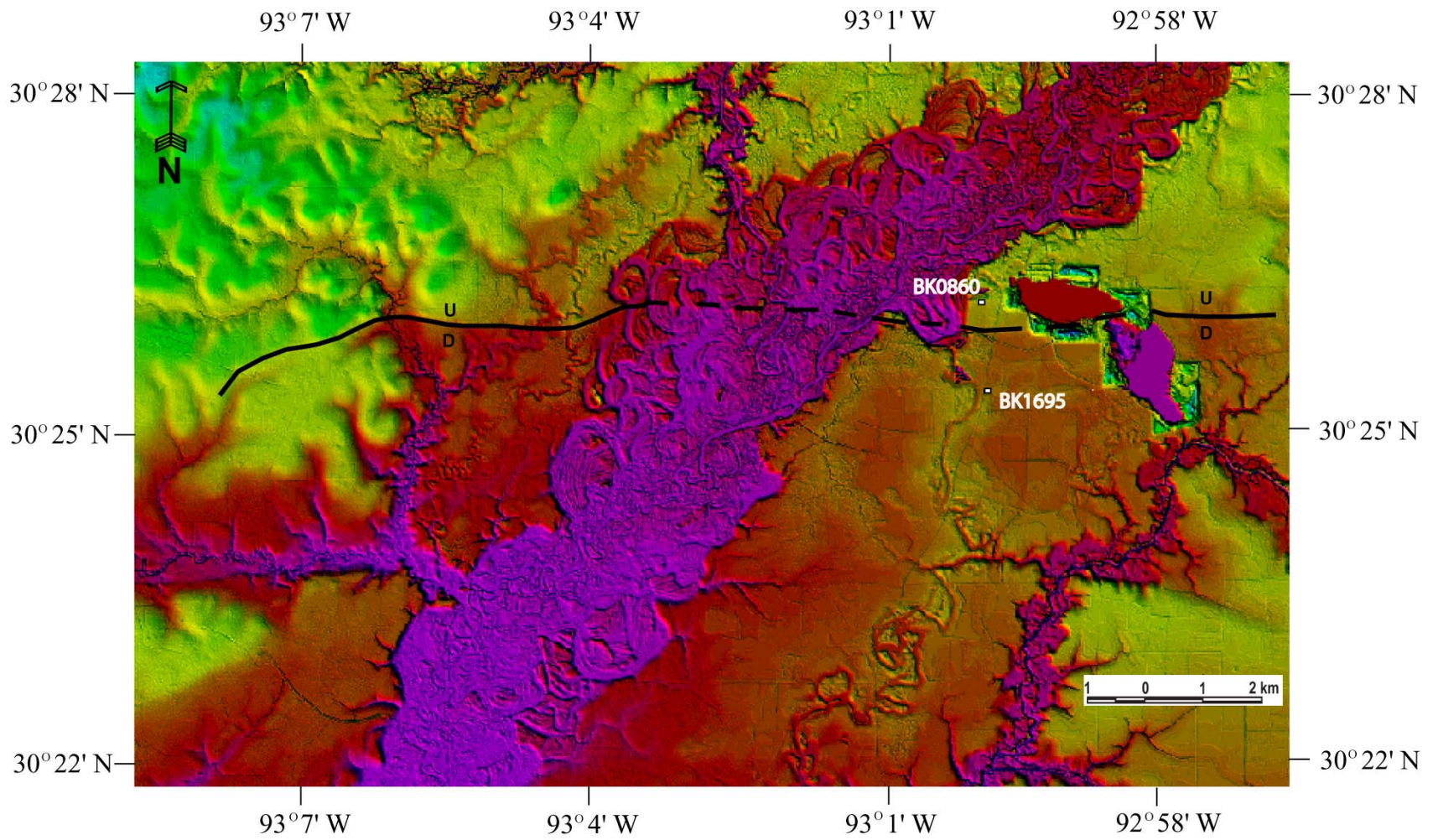


Figure 4.3. The Indian Village fault-related step and adjacent benchmarks.

4.1.2 Iowa Area

The east-west trending topographic step seen in Figure 4.4 is downthrown to the north and ranges in height from 0.5 m to 2.5 m. Evidence of the offset created by this feature consists of drainage pattern control, displacements in roadways, and truncation of older terrace features. This step appears to be the surface expression of a major down-to-the-north normal fault associated with the Iowa, Woodlawn and Welsh salt structures. Several subsurface studies have mapped this normal fault (Atwater and Forman, 1959; Paine, 1962; Pyle and Babisak, 1951; Hickey and Sabate, 1972; Wallace, 1966; Bebout and Gutierrez, 1983), which corresponds well in location and morphology with the Iowa fault-related step. Atwater and Forman (1959) reported that the Iowa salt dome experienced a phase of post-Miocene uplift which created displacement along this fault that could be traced to within 500 meters of the ground surface.

Because there were two separate leveling lines that crossed this fault near Iowa, we were able to compute rates for a pair of transects across the fault. The western transect connected benchmarks BK1679 to BK1680 along state Highway 308 and the eastern transect connected benchmarks BK0756 and BK0753 along state Highway 165. The height difference between benchmarks BK1679 and BK1680 was 7.14561 m in 1969 and 7.1716 from 1986 leveling. These values give a change in elevation of 0.02599 m, which equals a vertical slip rate of 1.5 mm/yr for this western transect across the fault. Unfortunately, these benchmarks could not be recovered and consequently no recent leveling could be performed along this transect. The benchmarks that provide vertical control along the eastern transect were leveled to in 1955 and 1970 and also at the beginning of 2005 as part of this thesis project. The relative height difference obtained between these two benchmarks was 1.40218 m in 1955 and 1.41197 m in 1970. These numbers equate to a relative height change of 0.00979 m or 9.8 mm during that span. This change amounts to a very low rate of 0.66 mm/yr of normal movement across this portion of the Iowa fault. We leveled to the same benchmarks again in early 2005 to attempt to quantify the fault motion since the benchmarks were last surveyed in 1970. This leveling run yielded a height difference of

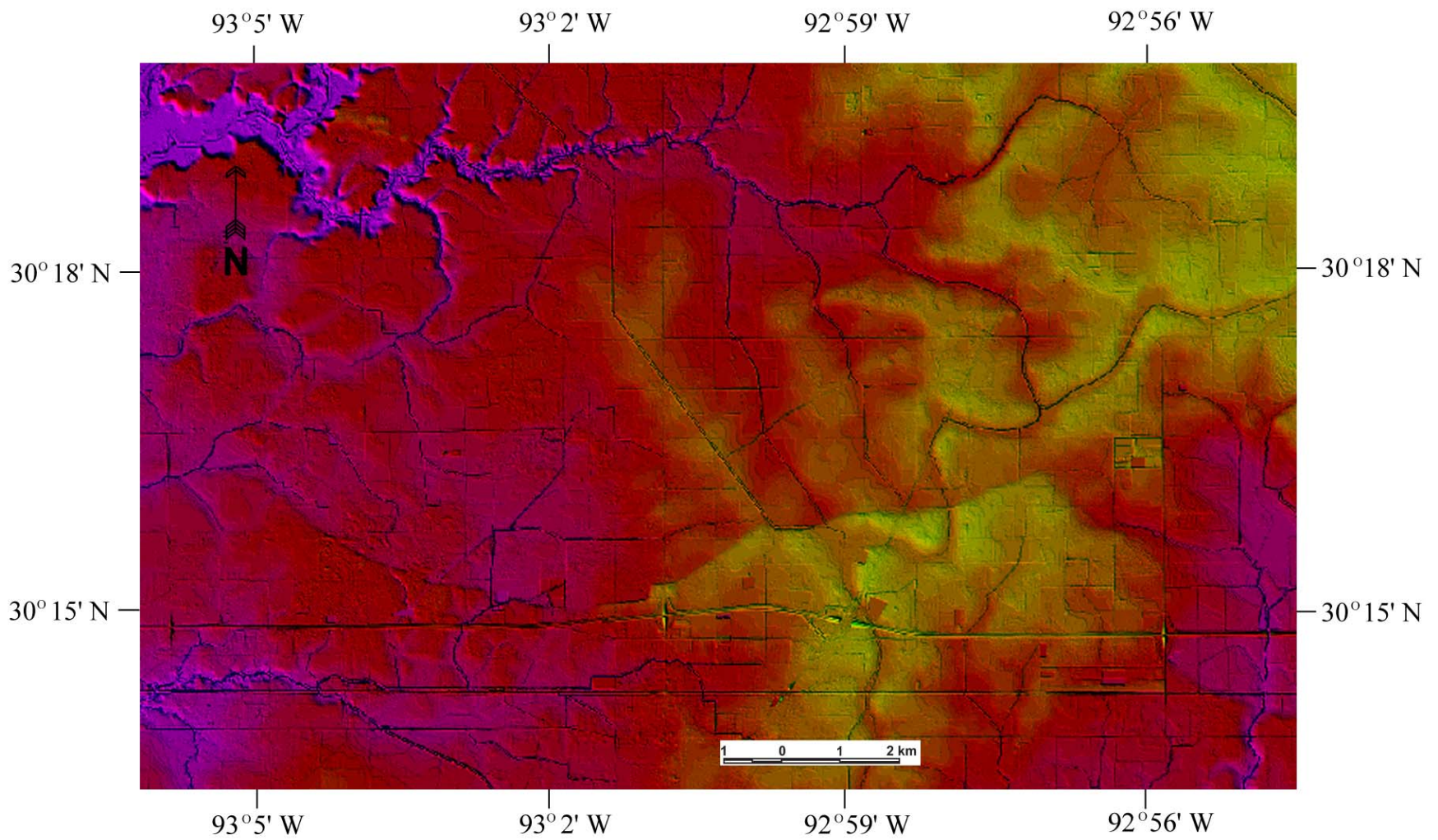


Figure 4.4. Uninterpreted LIDAR image of the Iowa area.

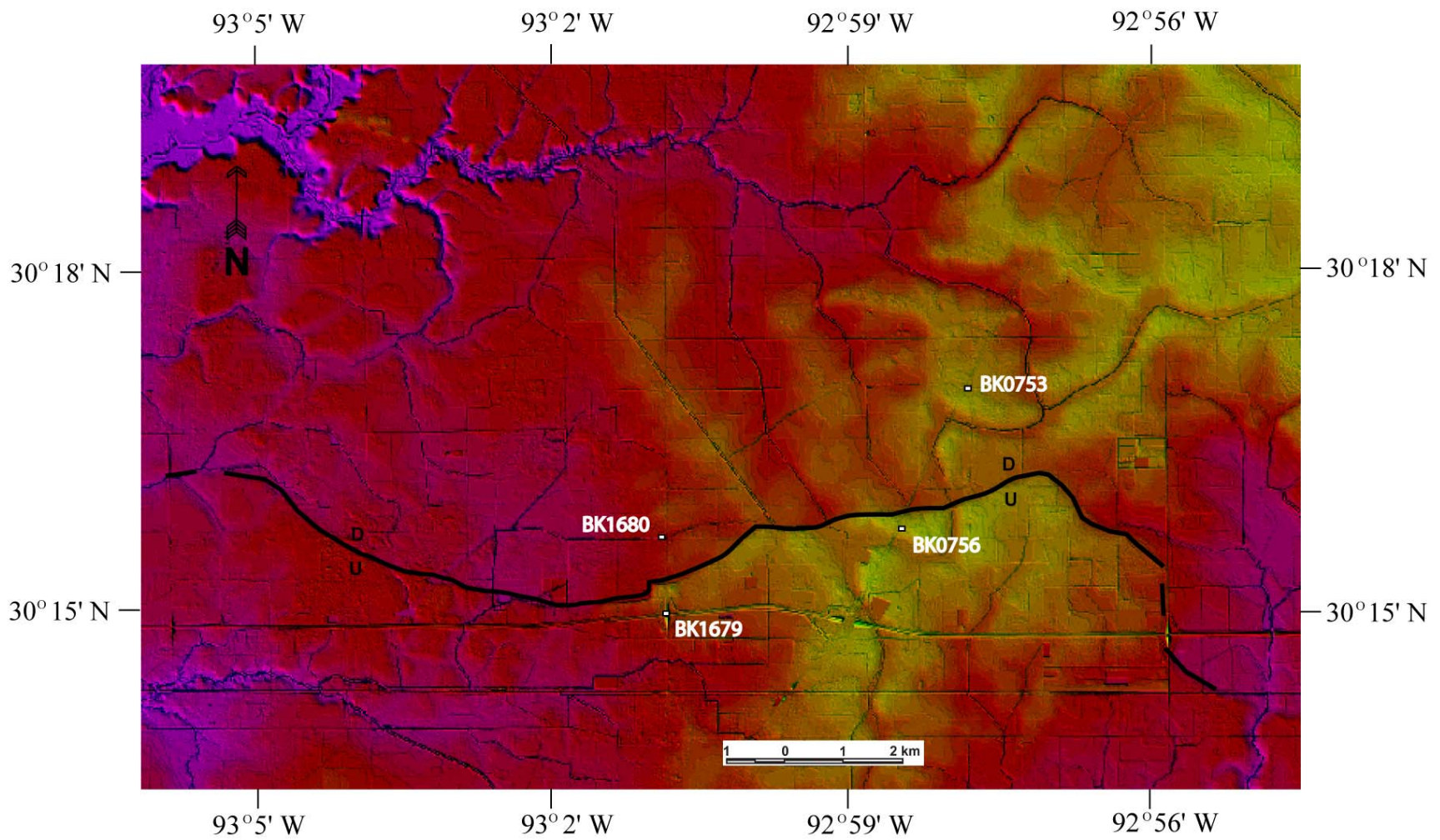


Figure 4.5. The Iowa fault-related step and adjacent benchmarks.

1.38316 m between the benchmarks, a change of 0.02881 m since the previous leveling run. However, this displacement implied a reversal in vertical movement, since benchmark BK0753 on the downthrown side of the fault moved up relative to BK0756 on the upthrown side of the fault. It should be noted that this reversal in motion was relatively slow at only 0.83 mm/yr for the period 1970 to 2005.

4.1.3 Moss Lake Area

The conspicuous topographic feature in Figure 4.6 located just south of Lake Charles crosses the Calcasieu River and is termed here the “Moss Lake fault-related step”. This feature is suspected to be the surface expression of a regional growth fault that has been mapped from well data by several workers (Codina, 1964; Hickey and Sabate, 1972; Wallace, 1966; Bebout and Gutierrez, 1983). The fault is part of the larger Lake Arthur Fault System and is associated here with the East Moss Lake and Bayou Choupique oil and gas fields. The location, morphology, and motion associated with this geomorphic step strongly suggest it is indeed the surface expression of this well-known subsurface fault. The surface displacement created by this fault-related step is relatively subtle (0.5 to 1.5 meters) although field observations have found evidence of offset in roadways and the ground surface in the Moss Lake area associated with its active movement. This feature apparently extends westward across the Calcasieu Ship Channel where it truncates the Pleistocene terrace near Bayou Choupique (Heinrich, 2000; Snead et al., 2002).

The Moss Lake fault-related step, just to the east of the Calcasieu River, was leveled across in 1965 and 1982 and was also re-leveled at the end of 2004 as part of the fieldwork for this thesis. The 1965 leveling data for benchmarks BK1508 and BK1509 show elevations for these control points of 2.60963 m and 4.17337 m respectively. This yields a relative height difference between the benchmarks of 1.56374 m for this leveling run. The field elevations of these benchmarks in 1982 were 2.58089 m and 4.04275 m providing a height difference of 1.46186 m at this time. The change in height between these vertical monuments during the period 1965 to 1982 was thus, 0.10188 m or 101.88 mm. This value equals an average vertical slip rate

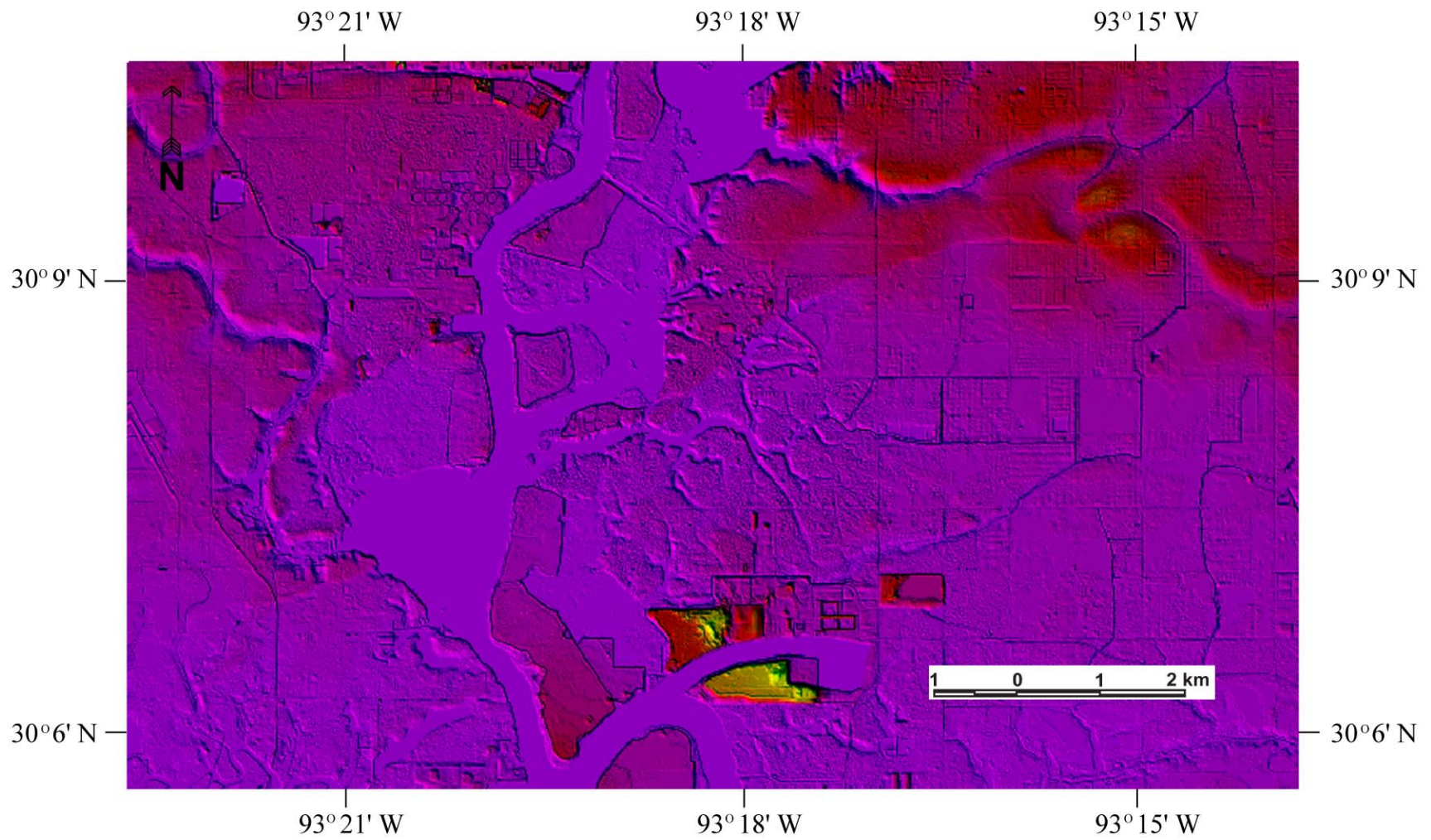


Figure 4.6. Uninterpreted LIDAR image of the Moss Lake area.

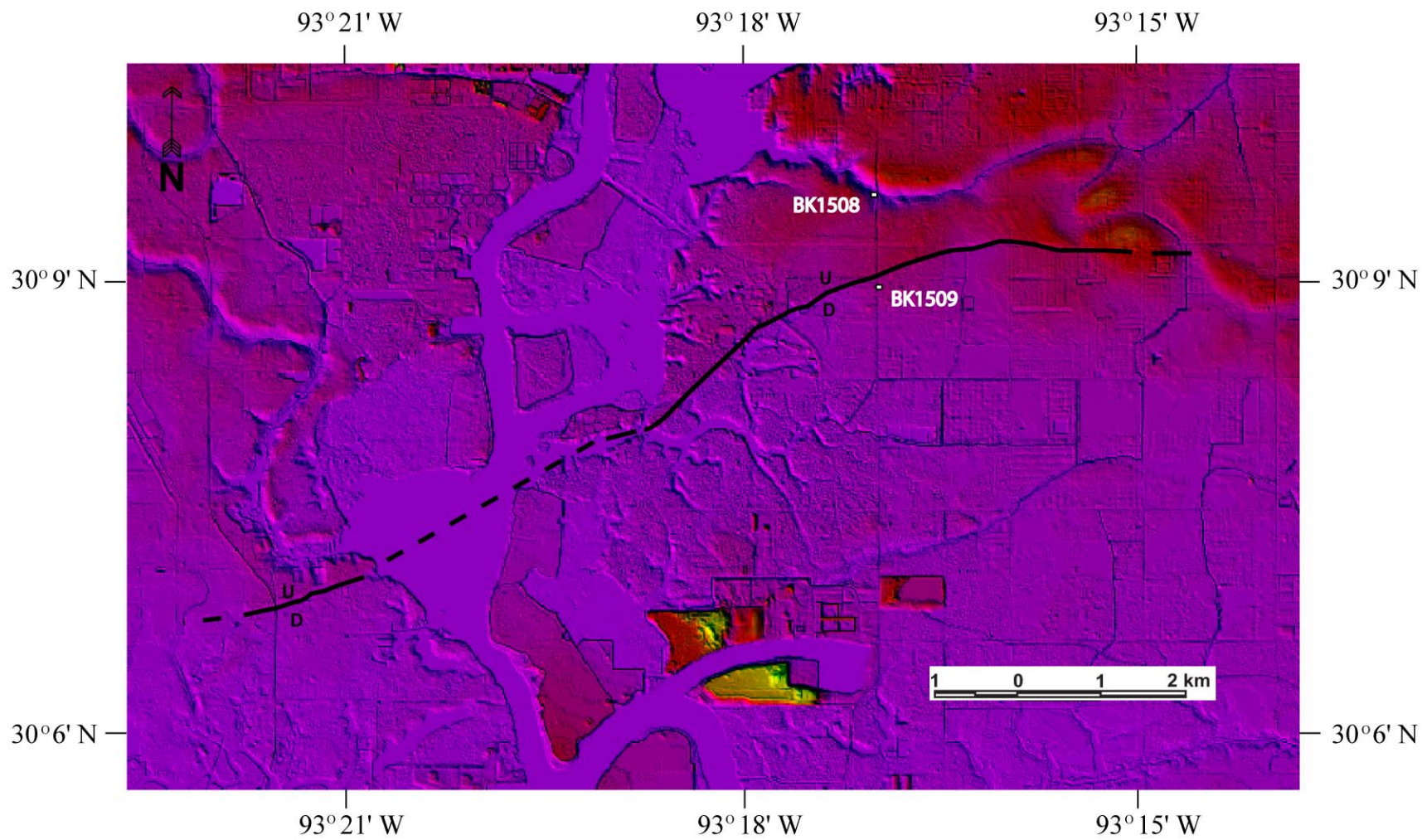


Figure 4.7. The Moss Lake fault-related step and adjacent benchmarks.

for this epoch of 6.0 mm/yr across the Moss Lake fault-related step. The leveling that we performed resulted in a height difference of 1.44087 m, which by comparison to the 1982 data, shows that benchmark BK1509 had since moved down 20.9 mm relative to BK1508. This displacement, when averaged over the 23 years between leveling runs, equals a rate of 0.95 mm/yr of normal vertical slip on this fault.

4.1.4 Vinton Area

There are numerous faults that extend out radially from the Vinton salt dome and it appears a few of those faults reach the ground surface. LIDAR imagery clearly shows that at least three topographic steps traverse through the area near Vinton. A gravity analysis of this area (Wilson and Noel, 1983) showed the existence of a saddle (gravity high) connecting the Vinton Dome and the Edgerly Dome. This suggests the domes have shared a similar structural evolution, which could be the cause of the faulting that correlates with these surface features. Subsurface mapping by Levie (1985) shows a fault which projects out from the Vinton salt dome in a northeasterly direction and bifurcates in a manner similar to that exhibited by the topographic steps. The two Vinton fault-related steps that were investigated in this study are identified on the LIDAR images (Figure 4.8) and are termed here, the “East Vinton fault-related step” and “West Vinton fault-related step”. These features are associated with offsets in roadways such as Interstate 10, US Highway 90, and State Highway 108 near the Vinton area. The more prominent of the two steps is the western one that extends in an arcuate pattern from near the Vinton salt dome to the area near the Edgerly Dome. As evidenced by the LIDAR images, the nature of the movement along this fault is quite unique in that along the southern portion of this fault the western block is downthrown whereas for the northern part the opposite is the case. The shorter East Vinton fault-related step exhibits relatively less surface offset (0 to 1 m) compared to the West Vinton fault-related step, which measures up to 2 meters in height.

Several leveling lines along US Hwy 90 crossed the northern portion of the West Vinton fault-related step over the past 50 years and this data provides the basis for the following

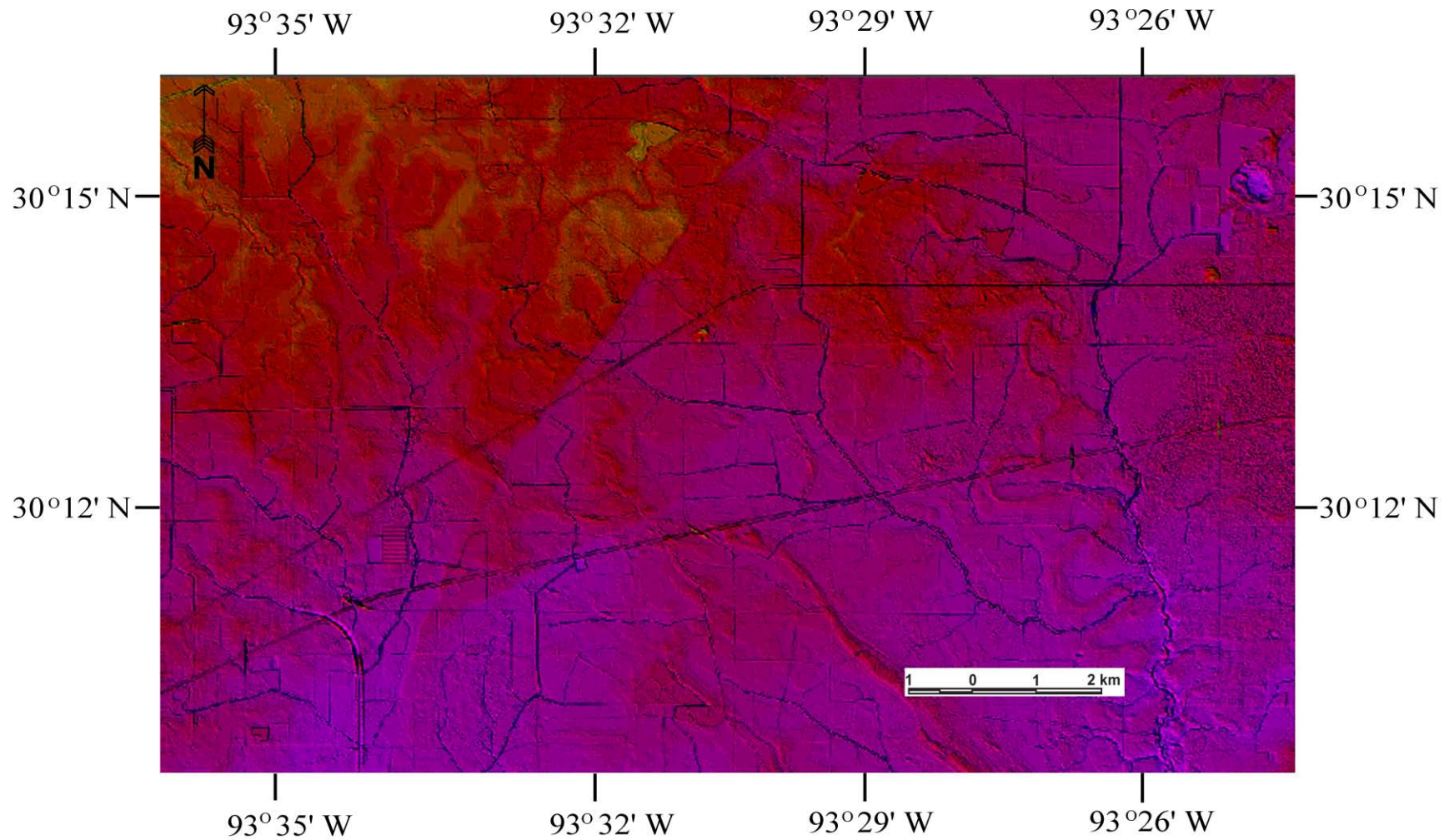


Figure 4.8. Uninterpreted LIDAR image of the Vinton area.

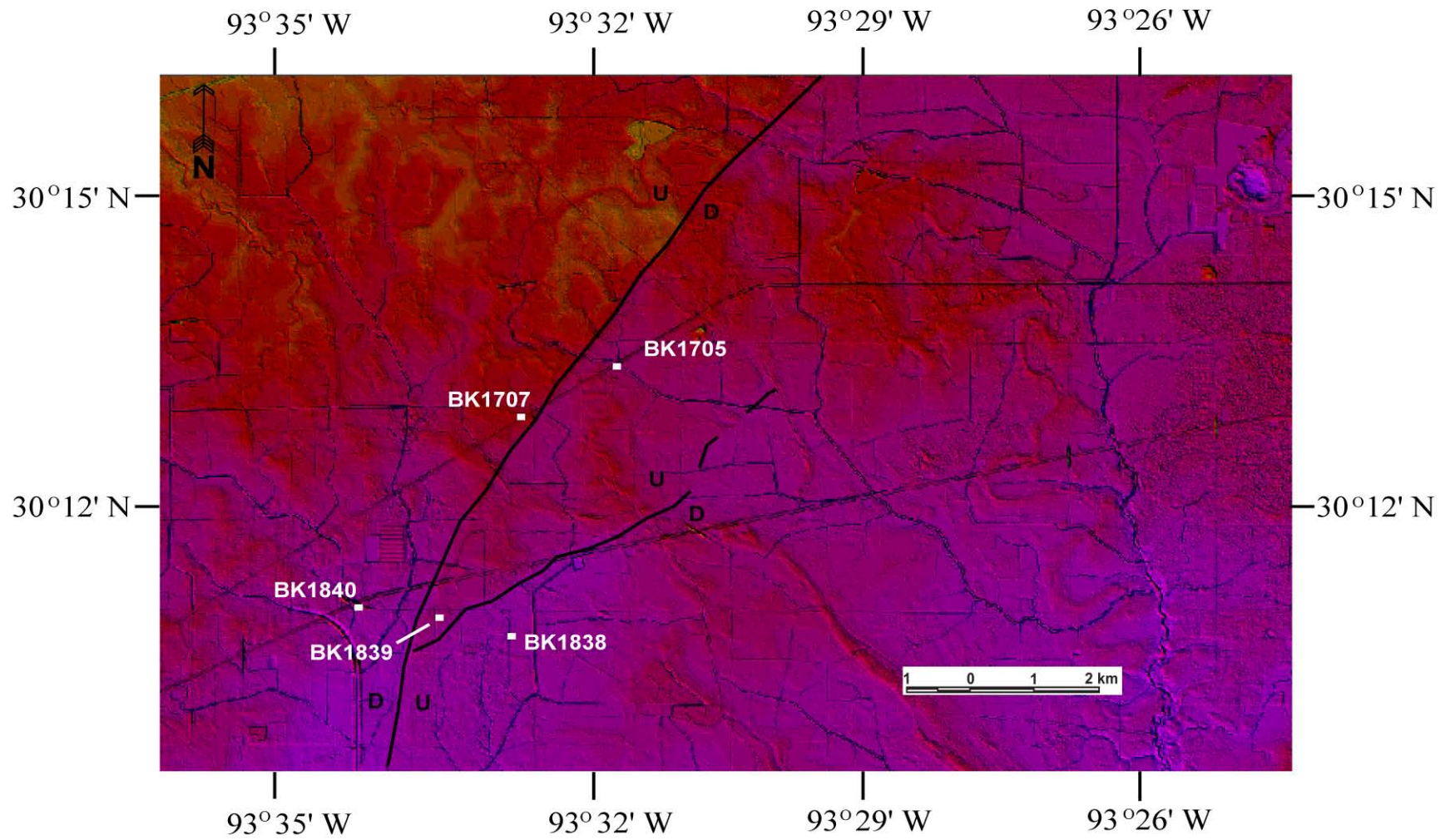


Figure 4.9. The Vinton fault-related steps and adjacent benchmarks.

kinematic analysis. The height difference between benchmarks BK1707, which lies on the upthrown block, and BK1705, which sits on the downthrown one, was measured as 0.46649 m from leveling done in 1955. This difference was then determined to be 0.53329 m when leveled in 1972, a change of 0.0668 m over that 17 year span. This equates to a rate of movement across this transect of 3.8 mm/yr for the epoch 1955 to 1972. These benchmarks were again leveled to in 1982 and at that time a height difference of 0.54155 m was measured. From this value, a change in relative benchmark height since the previous leveling run in 1972 is calculated as 0.00826 m. When averaged over the 10 years between levelings, this change equals a 0.92-mm/yr rate of slip along the fault for that period. In 1986 these benchmarks were leveled to again and at this time a height difference of 0.56687 m was measured. This equates to a change of 0.02352 m and a vertical slip rate of 5.85 mm/yr for the period 1982 to 1986. For this thesis project, we performed additional leveling runs along this transect in order to update these rates with respect to current benchmark positions. The height difference determined from our 2005 leveling was 0.56574 m, a decrease of 1.13 mm since the last leveling run in 1986. This shows that not only did the fault cease to continue its trend of previous motion, but a slight reversal of slip was detected at a rate of 0.06 mm/yr since 1986.

For the southern portion of this fault segment, benchmark BK1840 is located on the downthrown western block and BK1839 is on the eastern upthrown one. These benchmarks were leveled to in 1970 and at this time a height difference of 7.64434 m was measured. Subsequent leveling in 1982 determined a height difference of 7.59658 m, which amounts to a change of 0.04776 m, with BK1840 moving down relative to BK1839. This displacement equals a slip rate of 4.06 mm/yr for the period between the leveling runs in 1970 and 1982. In order to obtain a current rate of movement for this portion of fault, we leveled between these same benchmarks near the end of 2004. This fieldwork resulted in a height difference of 7.53295 m, a change of 0.06363 m since the previous leveling in 1982. This shows that from 1982 to 2005, these benchmarks continued their previous relative movement, but at a rate of 2.76 mm/yr.

Only one vertical slip rate could be computed for the smaller eastern fault segment near Vinton because there was only a single previous leveling line that crossed the fault in 1970. For this fault, benchmark BK1839 occupies the upthrown side while BK1838 lies on the downthrown fault block. A height difference of 0.61481 m was determined between these benchmarks from the leveling performed in 1970. We then re-leveled this transect across the fault-related step in late 2004 in order to compute a current rate of movement. Our leveling resulted in a height difference of 0.63867 m, which equates to a change in the height difference between these benchmarks of 0.02386 m. This value gives us a relatively low rate of normal motion of 0.69 mm/yr between 1970 and 2005.

4.1.5 Sulphur Area

The linear topographic feature in Figure 4.10 traverses northwesterly through the residential and commercial areas of Westlake and Sulphur, Louisiana. A review of the literature has failed to locate any evidence of a subsurface fault that may correlate with this geomorphic step. However, there is abundant evidence that this feature is associated with a currently active fault. Damage to roadways, homes, sidewalks and businesses can be found all along the trace of this fault suggesting ongoing deformation. A portion of this fault-related step, which measures 0.5 to 1.5 m in height, was identified by Louisiana Geological Survey on their geologic map of the Lake Charles area (Snead et al., 2002). Although this feature could not be tied to a subsurface fault, the observation that it runs from the Lockport salt dome to the Sulphur Mines dome indicates that it is likely an ancient geologic feature experiencing active motion.

Although numerous benchmarks are located in the area around Sulphur, LA, a large number of them have been destroyed due to construction of new homes and businesses. This creates a problem whereby the benchmarks that have provided the best vertical control around faults in recent history can no longer be used for computing displacements and rates of fault motion. There are two major leveling transects that cross the Sulphur fault-related step, one along US Hwy 90 and a second along state Hwy 27. For the eastern transect, which runs north to

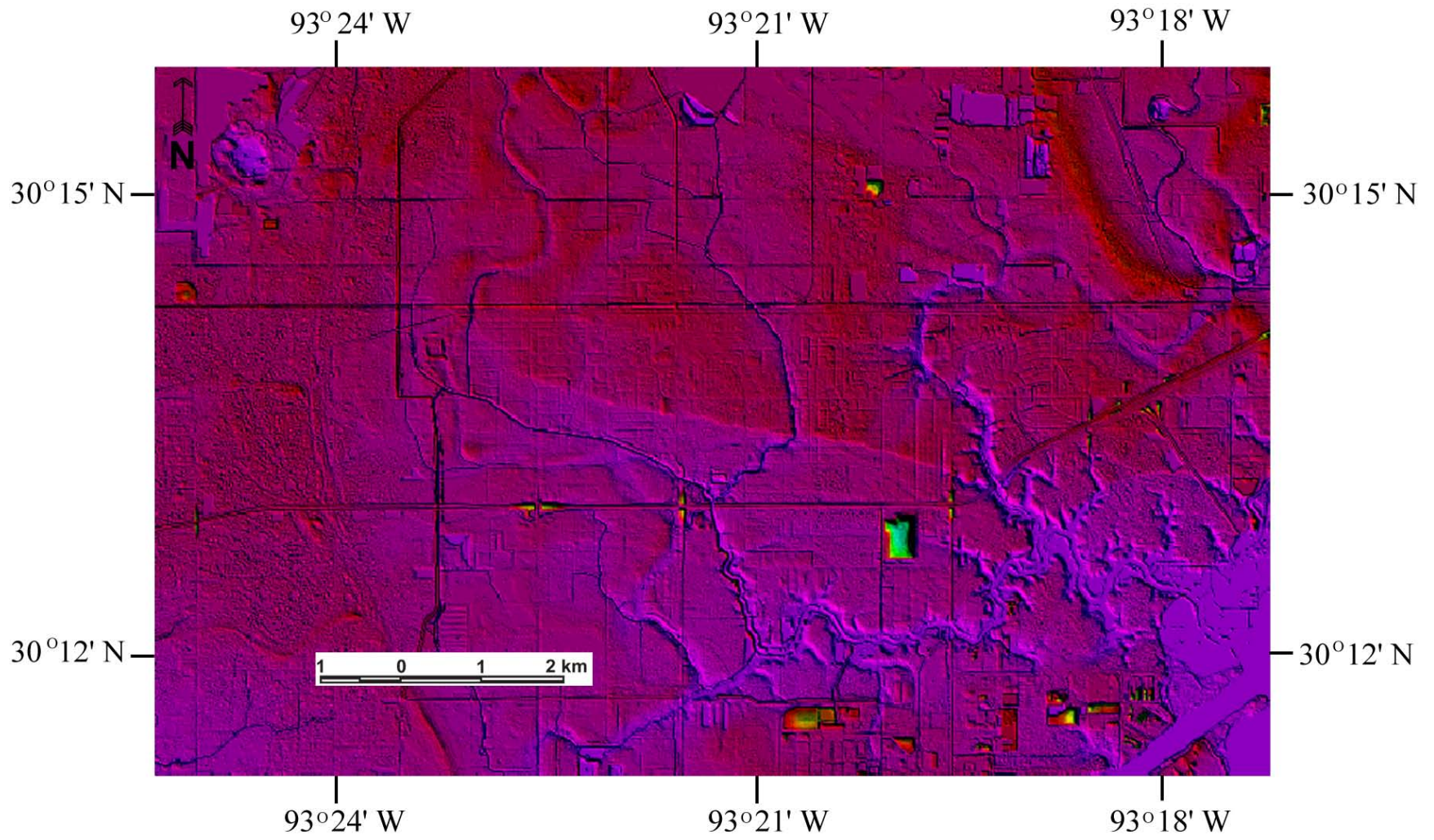


Figure 4.10. Uninterpreted LIDAR image of the Sulphur area.

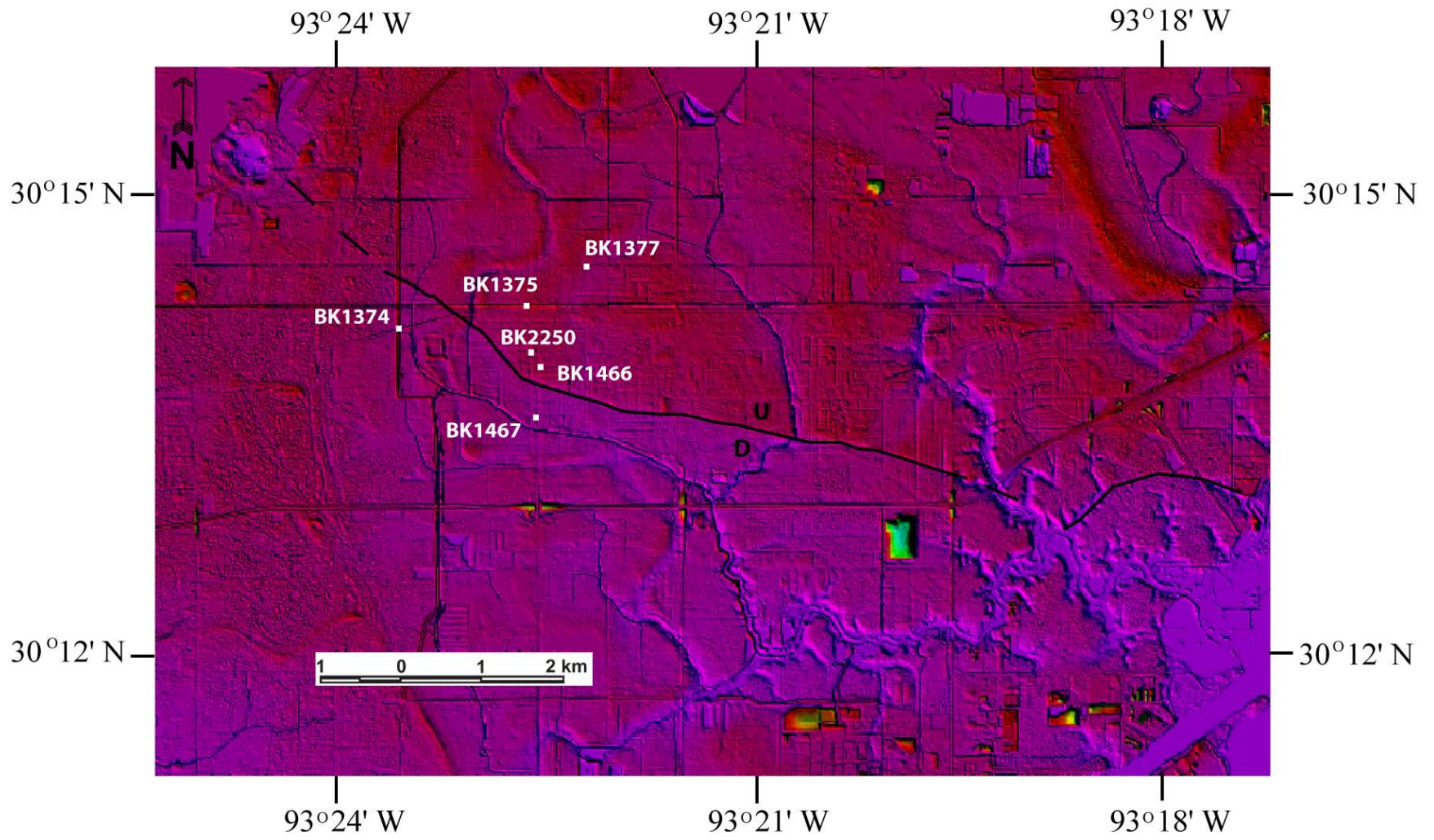


Figure 4.11. The Sulphur fault-related step and adjacent benchmarks.

south along Hwy 27, benchmark BK1467 provides vertical control for the downthrown block. Two benchmarks on the upthrown block, BK1375 and BK1466, have been destroyed, but data obtained from leveling to them before their destruction has provided historical displacements and rates along this transect.

The height difference between benchmarks BK1466 and BK1467 was measured as 1.2251 m from leveling in 1965. Subsequent leveling at the end of 1972 found this difference to then be 1.26715 m, a change of 0.04205 m. This change amounts to a rate of vertical displacement of 5.54 mm/yr for the time period of 1965 to 1972. This was the only kinematic data that could be computed for these benchmarks because BK1466 was subsequently destroyed. That same project in 1965 also visited BK1375 and a height difference between that benchmark and BK1467 was found to be 2.63067 m. The 1972 line also visited BK1375 and at this time a height difference of 2.66128 m was measured, equating to a change of 0.03061 m. This vertical displacement between benchmarks adjacent to the step allows us to compute a 4-mm/yr rate of vertical slip between 1965 and 1972. A leveling project in 1982 also visited these two benchmarks and at this time a height difference of 2.68827 m was recorded. This amounts to a relative height change since the previous leveling of 0.02699 m, which equals a rate of 2.92 mm/yr for the period between levels in 1972 and 1982. The only currently existing benchmark that could be used to determine displacements along this transect was BK2250, which is located near where BK1466 had been positioned. This benchmark was leveled to as part of the 1982 project and a height difference of 1.47032 m was measured between BK2250 and BK1467. Leveling performed at the end of 2004 as part of this thesis project then determined that the height difference was 1.47561 m. This amounts to very slight increase in relative benchmark heights of 5.29 mm since the 1982 leveling. Obviously this minimal change shows that the fault has experienced a very low rate of movement of 0.23 mm/yr over the past 23 years.

By comparison, the line of levels that runs east-west along US Hwy 90 in Sulphur shows much lower historical displacements across the Sulphur fault-related step. This transect connects

benchmark BK1374 on the downthrown side of the fault to BK1377 on the upthrown side. It measures 2.35 km in length and was leveled in 1972, 1986, and again at the end of 2004 by the author. The 1972 leveling measured a 1.26207 m height difference between these benchmarks, while leveling in 1986 found the difference to be 1.27768 m. This relative change of 0.01561 m shows that the fault experienced vertical slip of 1.17 mm/yr along this transect from 1972 to 1986. In order to update this rate with respect to the current benchmark heights, we re-leveled this transect in November of 2004. This leveling resulted in a height difference of 1.28067 m, a change of 0.00299 m since the previous leveling in 1986. From this value, it was calculated that the vertical slip had slowed to a rate of only 0.16 mm/yr during the period of 1986 to 2005.

4.1.6 Moss Bluff Area

A geomorphic step that runs northeasterly through the Westlake and Moss Bluff areas is slightly visible on LIDAR imagery (4.12) and almost imperceptible in the field. A one-meter high step has been observed in the field near the Houston River in Westlake and a fault-related step of comparable height has been located near Moss Bluff. This topographic feature corresponds well in location and morphology with a fault mapped in the subsurface that runs from the Lockport dome to the Gillis-English Bayou area (Friedel, 1978). Despite the lack of definitive correlation with a subsurface fault, the observations that this feature appears to cause a diversion of the Houston River and exhibits relative vertical displacement measured by leveling data, suggest it is fault related.

Geodetic leveling to benchmarks that straddle this fault-related step has detected motion across it over the past three decades. The two benchmarks that were used to determine fault motion are BK1593 on the northern, upthrown side of the fault and BK1591 on the southern, downthrown block. Leveling performed in 1969 measured a height difference of 0.67178 m between these benchmarks, while a leveling run in 1986 found this difference to be 0.72991 m. This shows that these benchmarks experienced a relative vertical displacement of 0.05813 m between 1969 and 1986. This displacement amounts to a vertical slip rate of 3.35 mm/yr for the

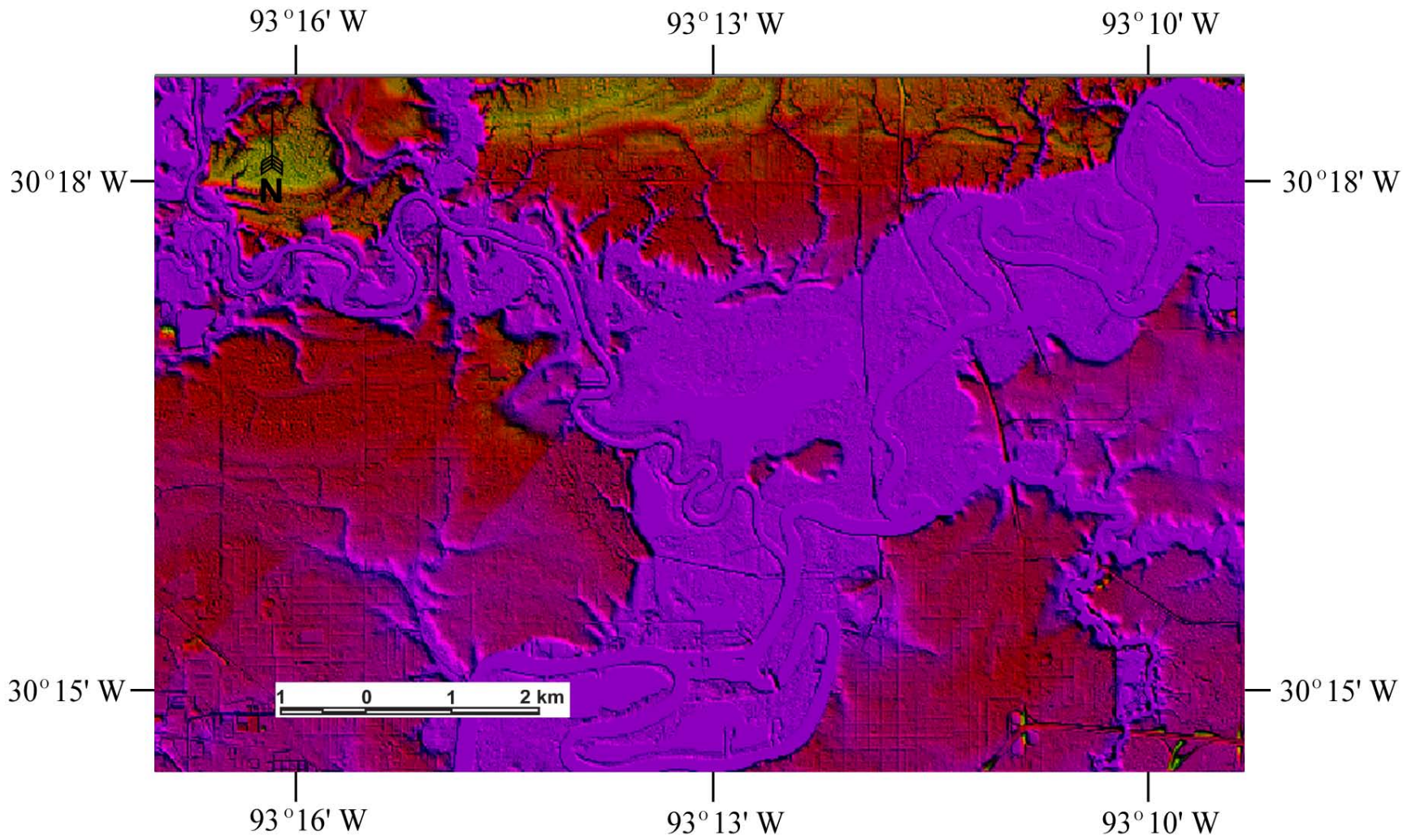


Figure 4.12. Uninterpreted LIDAR image of the Moss Bluff area.

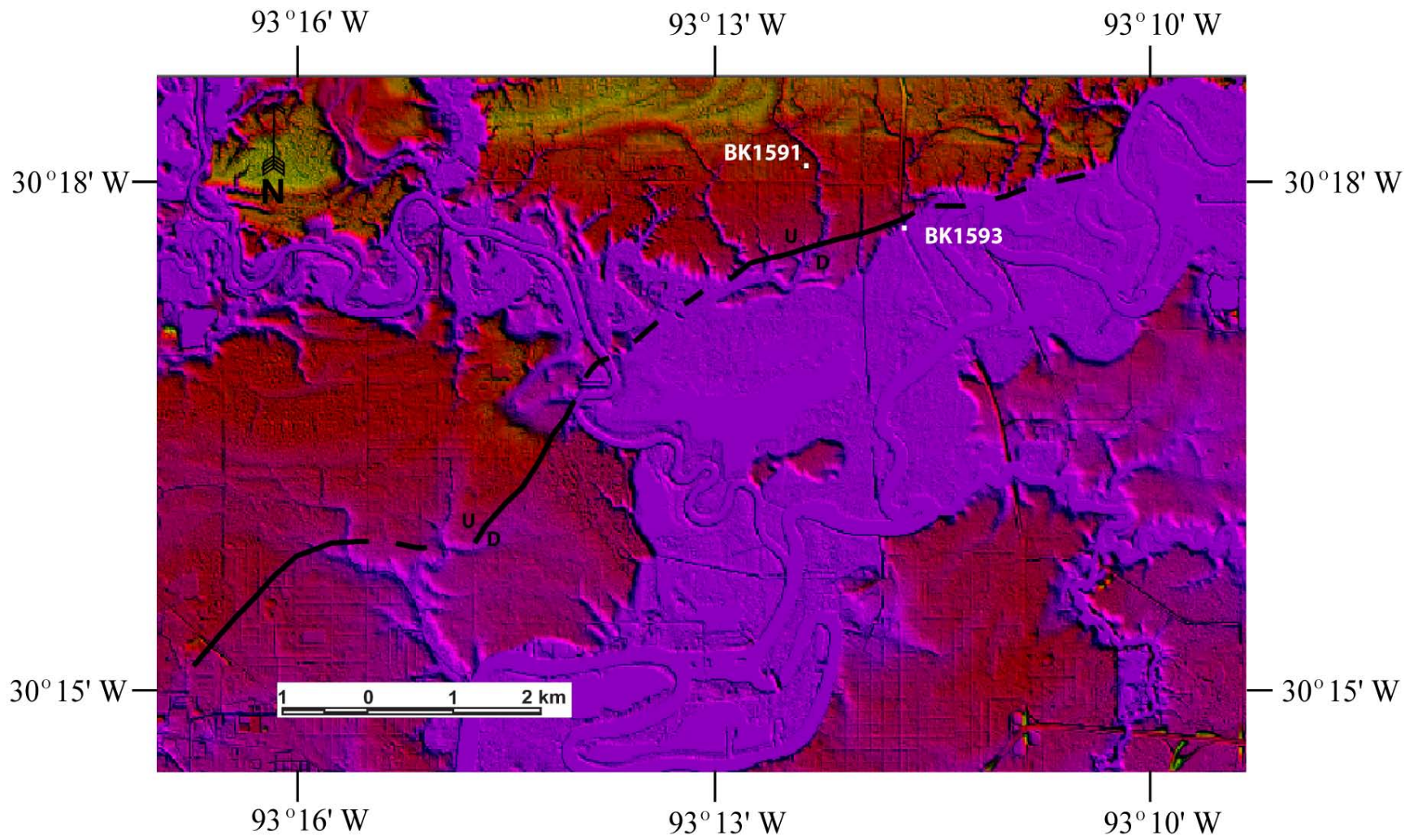


Figure 4.13. The Moss Bluff fault-related step and adjacent benchmarks.

Moss Bluff fault during that time span. We again leveled this transect between BK1593 and BK1591 near the end of 2004 to determine the current slip rate across this fault. At this time, a height difference between the benchmarks of 0.74183 m was measured, which equates to a change of 0.01192 m since the last survey in 1986. From this new leveling data, we calculated a vertical slip rate of 0.64 mm/yr for the period between 1986 and 2005.

4.1.7 DeQuincy Area

Due to the significant relief it creates (2 to 8 m), the DeQuincy fault-related step is easily mapped on LIDAR imagery (Figure 4.15). The fault is down-to-the-south, with the beds on the downthrown side dipping into the fault in a rollover pattern. This observation is in agreement with other previous studies of the DeQuincy fault and similar fault segments of the Tepetate Fault System (Heinrich, 2000; Snead et al., 2002). In the subsurface, this fault is a major down-to-the-south listric fault (Wallace, 1966, Hickey and Sabate, 1972; Kearby, 1989) and is associated with the DeQuincy, Perkins, and East Perkins oil and gas fields in Northern Calcasieu Parish. The fault-related step visible on the LIDAR is the surface expression of the “DeQuincy fault segment”, which is part of the larger Tepetate fault zone.

Unfortunately, the amount and quality of leveling data that crossed this fault was extremely poor and therefore no displacements or rates of motion could be calculated across it. In addition, the benchmarks that straddle the fault-related step could not be located or were destroyed, making it impossible to conduct new leveling transects across the DeQuincy fault-related step.

4.2 Calculation of Errors

Because this thesis deals solely with very precise height differences between two adjacent benchmarks and how those differences changed over time, the errors for the results obtained in this study are relatively small. Although the errors associated with geodetic leveling accumulate over the length of the line and can become substantial for long lines, the height differences obtained between nearby benchmarks are extremely precise. In order to calculate the errors for geodetic leveling data, one must

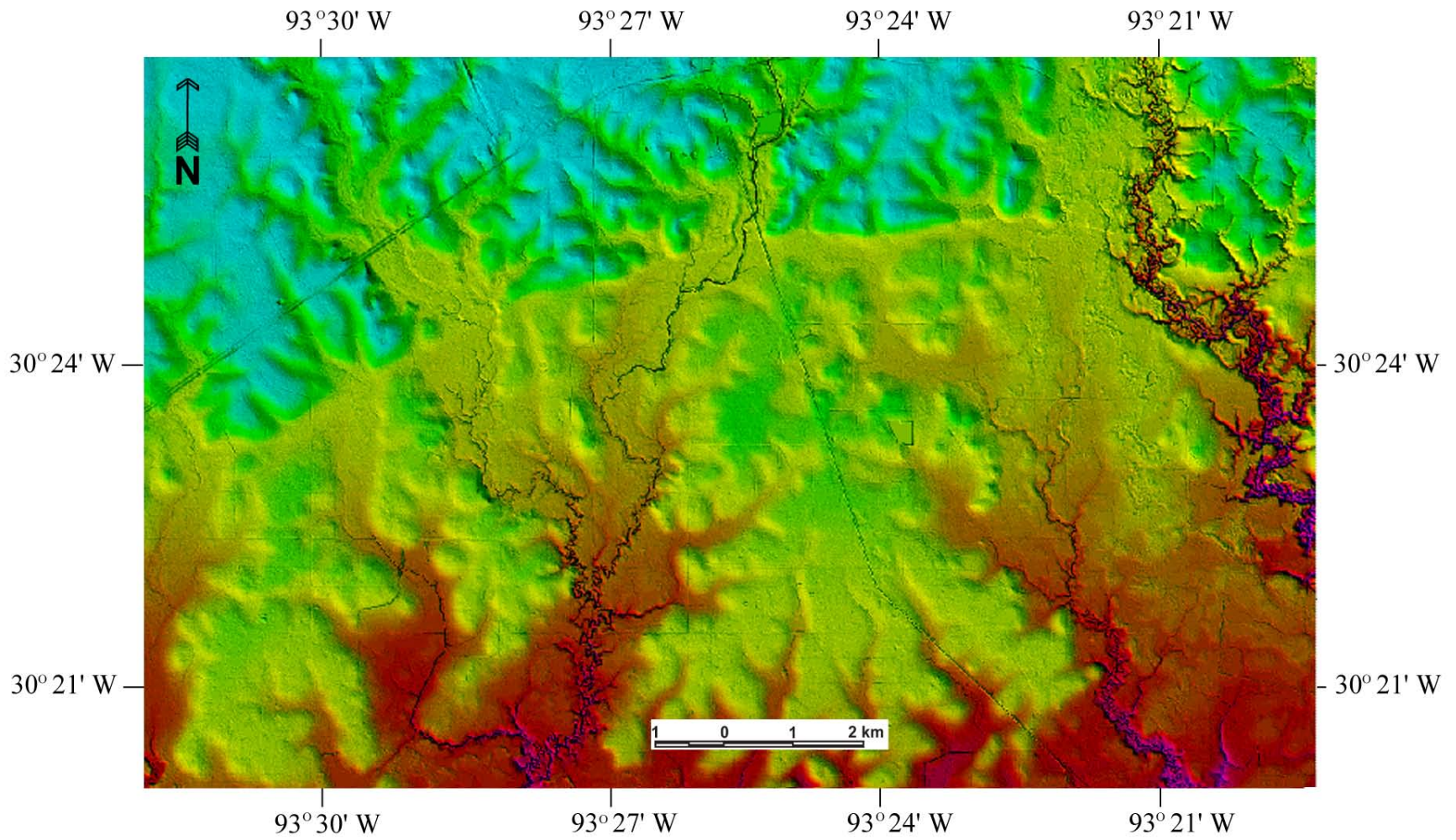


Figure 4.14. Uninterpreted LIDAR image of the DeQuincy area.

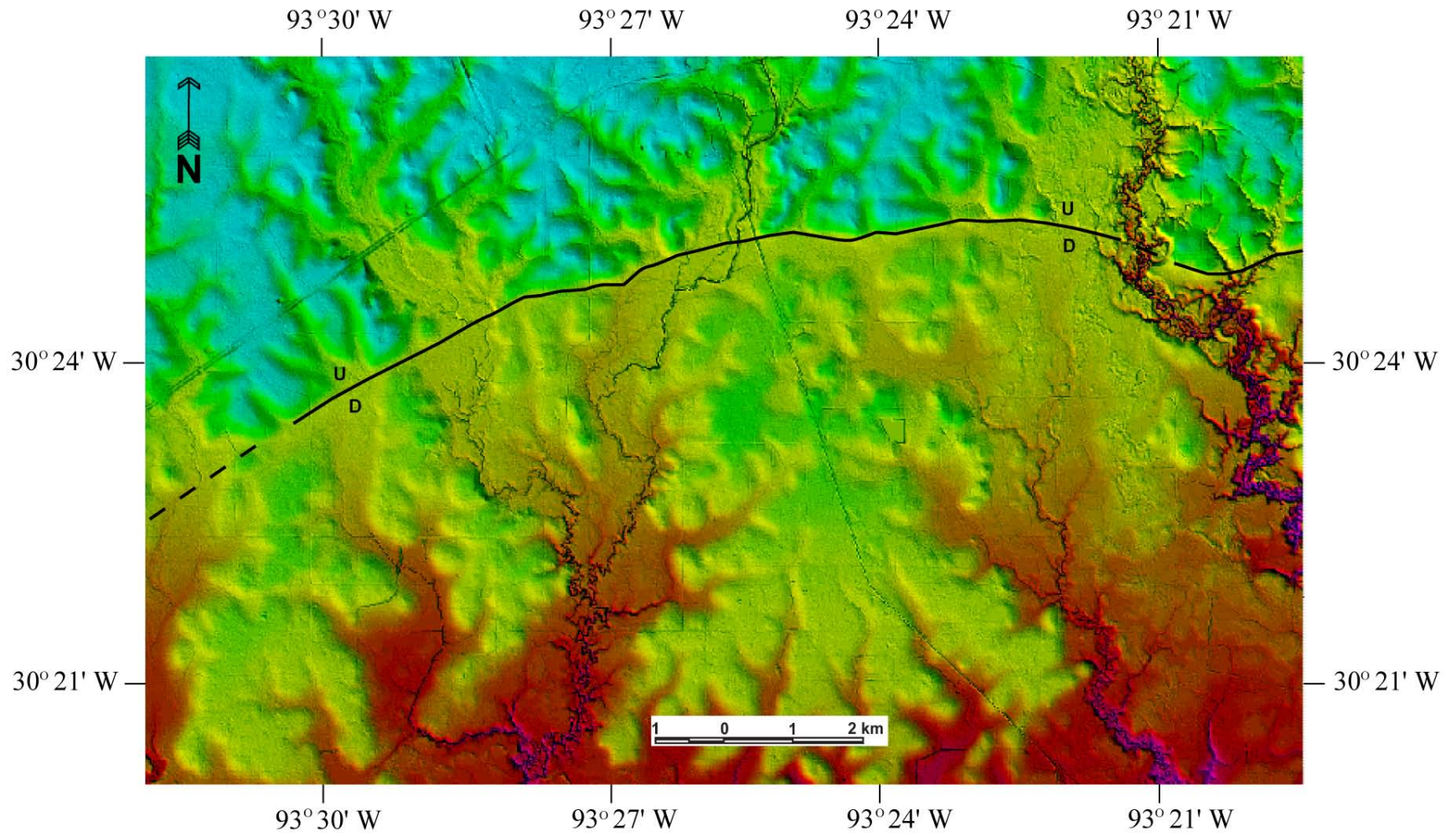


Figure 4.15. The DeQuincy fault-related step.

know the distance between the benchmarks surveyed as well as the order and class of the leveling lines. A simple formula for the precision of leveling, in millimeters is: $\alpha\sqrt{D}$, where **D** is equal to the distance between benchmarks in kilometers, and α is the standard deviation of leveling for 1 km (Holdahl, 1976). The values for α range from 0.5 for a 1st order, class I line to 2.0 for a 3rd order line (Bossler, 1984). This formula allows us to compute the precision of leveling between two points connected by a leveling line. In this thesis project, we calculated relative elevation changes and velocities by comparing height differences obtained in successive leveling runs. For the double-run levels that we performed, the errors for the height differences between benchmarks were taken as simply half of the closure obtained from the levelings. The total error for the relative vertical movement between benchmarks is then equal to the square root of the sum of the squares of the errors from both levelings. The above computation is not confused by discussion of systematic error since this error frequently tends to cancel for calculations of vertical movement since both levelings are normally performed over identical terrain and at nearly the same time of year (Holdahl, 1976). As evidenced by the errors computed in Table 4.1, repeated geodetic leveling can provide very precise values for relative height change between adjacent benchmarks.

4.3 Summary of Results

Table 4.1 Summary of results

Location	Benchmarks ¹ HW FW	Distance (km)	Epoch	Displacement ² (mm)	Error (mm)	Vertical Slip Rate ² (mm/yr)	Error (mm/yr)
Indian Village	BK1695-BK0860	1.48	1969 to 1986	61.18	±1.61	3.58	±0.10
Iowa - E	BK0753-BK0756	1.12	1955 to 1970	9.79	±0.41	0.66	±0.03
	BK0753-BK0756	1.12	1970 to 2005	-28.81	±0.92	-0.83	±0.03
Iowa - W	BK1680-BK1679	1.27	1969 to 1986	25.99	±1.38	1.52	±0.08
Moss Lake	BK1509-BK1508	1.06	1965 to 1982	101.88	±0.52	6.00	±0.03
	BK1509-BK1508	1.06	1982 to 2005	20.99	±0.49	0.95	±0.02
Vinton - S	BK1840-BK1839	1.35	1970 to 1982	47.76	±1.47	4.06	±0.13
	BK1840-BK1839	1.35	1982 to 2005	63.63	±0.67	2.76	±0.03
Vinton - S	BK1838-BK1839	1.52	1970 to 2005	23.86	±1.29	0.69	±0.04
Vinton - N	BK1705-BK1707	1.82	1955 to 1972	66.80	±0.67	3.80	±0.04
	BK1705-BK1707	1.82	1972 to 1982	8.26	±0.67	0.92	±0.07
	BK1705-BK1707	1.82	1982 to 1986	25.32	±0.89	5.85	±0.21
	BK1705-BK1707	1.82	1986 to 2005	-1.13	±0.59	-0.06	±0.03
Sulphur-E	BK1467-BK1375	1.37	1965 to 1972	30.61	±0.51	4.03	±0.07
	BK1467-BK1375	1.37	1972 to 1982	26.99	±0.51	2.92	±0.06
	BK1467-BK2250	0.89	1982 to 2005	5.29	±1.13	0.23	±0.05
	BK1467-BK1466	0.76	1965 to 1972	42.05	±0.28	5.54	±0.04
Sulphur-W	BK1374-BK1377	2.35	1972 to 1986	15.61	±0.87	1.17	±0.07
	BK1374-BK1377	2.35	1986 to 2005	2.99	±0.60	0.16	±0.03
Moss Bluff	BK1593-BK1591	1.45	1969 to 1986	58.13	±1.58	3.35	±0.09
	BK1593-BK1591	1.45	1986 to 2005	11.92	±0.39	0.64	±0.02

¹ - Permanent Identifiers (PIDs) for benchmarks in transect; HW = Hanging wall, FW = Footwall

² - positive values represent normal motion; negative values represent reverse motion

CHAPTER 5 DISCUSSION

5.1 Nature of Active Faulting

The leveling data presented above, along with the topographic mapping, field observations, and subsurface evaluation, provides substantial evidence of neotectonic activity in this part of southwest Louisiana. By integrating remote sensing imagery and structural mapping, numerous geomorphic steps in the study area were shown to represent the surface expression of active faults. Analysis of historical heights of vertical control points adjacent to these features has facilitated the calculation of displacements and rates of fault motion.

From the results in Table 4.1, we can make several observations regarding the nature of recent fault activity in the study area. Although it is evident from the benchmark displacements that these faults have moved at varying rates, the time ranges for the kinematic data and the possibility of human influences on faulting do not permit an evaluation of the hypothesis that faulting in the study area is episodic. Displacement along most of these faults was normal motion where the hanging wall benchmarks moved down relative to those on the footwall side. However, benchmarks in the East Iowa and North Vinton transects, showed displacement opposite that of the natural normal motion of these faults. Both instances of reverse motion were computed by comparison of height differences recently obtained by the author and those obtained in previous levelings. This brings up the issue of temporal variations in fault motion and the discussion of causes for those variations. A review of the displacements and rates shows that apparently these faults were more active in the 1960's and 1970's than they were prior and subsequent to that time. The average vertical slip rate on the faults in the study area was nearly 4 mm/yr in 1970, while in the past decade the average rate is less than a millimeter a year. A recent reduction in the rates of normal fault motion was measured and in the case of those two previously mentioned leveling transects, slight reversal of motion was detected. Understanding the reasons for this decrease in fault activity requires a discussion about the possible driving forces of neotectonics in the area.

5.2 Causes of Recent Fault Activity in Study Area

This research project aimed to resolve the issue of whether faulting in the study area was the result of human influence or natural causes. Since it has been demonstrated that most of the geomorphic steps in the area are the surface expressions of known subsurface faults, natural geologic forces obviously play some part in driving this current fault activity. These faults owe their origins to the accumulation and basinward sliding of thick sedimentary masses (Murray, 1961; Bruce, 1973) above a mobile substratum of salt and/or shale (Worrall & Snelson, 1989). Increased rates of sediment loading in the Northern Gulf of Mexico since Pleistocene time has apparently caused renewed motion along some of the older Tertiary fault systems of the Gulf Coast. The lithospheric flexure and crustal extension resulting from this loading has reactivated faults in and around the study area as proposed by Nunn (1985) and observed by Heinrich (2000) and Hanor (1985). It also appears that salt movement is causing surface fault displacement, as evidenced by the close relationship between salt structures and some of the fault-related steps, especially in the central portion of the study area. The ongoing faulting and vertical movement of salt may be mechanisms that compensate for the extension and basinward sliding of the thick wedge of Cenozoic sediments toward the Gulf of Mexico above layers of mobile shale and salt.

Several workers claim that faulting is accelerated by anthropogenic causes around Houston, Texas, an area with a similar geologic setting to southwestern Louisiana. The relatively high rates of motion along faults computed in this study suggest that this recent fault activity may not be due solely to natural geologic causes. If the vertical slip rates computed above were characteristic of the motion along these features since they were formed, much higher fault-related steps should be present in the study area. Although, as discussed previously, Gulf Coast faults are known to move episodically and therefore it is possible that the period of increased fault activity in the 1960's and 1970's represents a phase of naturally high rates of faulting. Despite this consideration, the close temporal and spatial relationship between increased subsurface fluid withdrawal and accelerated faulting is interesting. Figure 5.1 compares the amount of

groundwater withdrawn from wells in Calcasieu Parish with the average vertical slip rates on faults for the past fifty years. Not only did faulting accelerate during the period of increased groundwater withdrawal, but also displacements along faults within the area of highest piezometric decline were greater than those in areas of lesser decline. During the late 1960's and early 1970's, when groundwater levels were at all-time lows, the average vertical slip rate on faults near the Lake Charles Industrial District was almost double that of faults in the outlying areas (Figure 5.2). Lowering of the piezometric surface in the study area, due to depressuring of aquifers, was associated with an increase in the natural motion of these faults. The following section will provide a more detailed discussion of subsurface fluid withdrawal in the thesis area and how this could possibly be related to accelerated faulting.

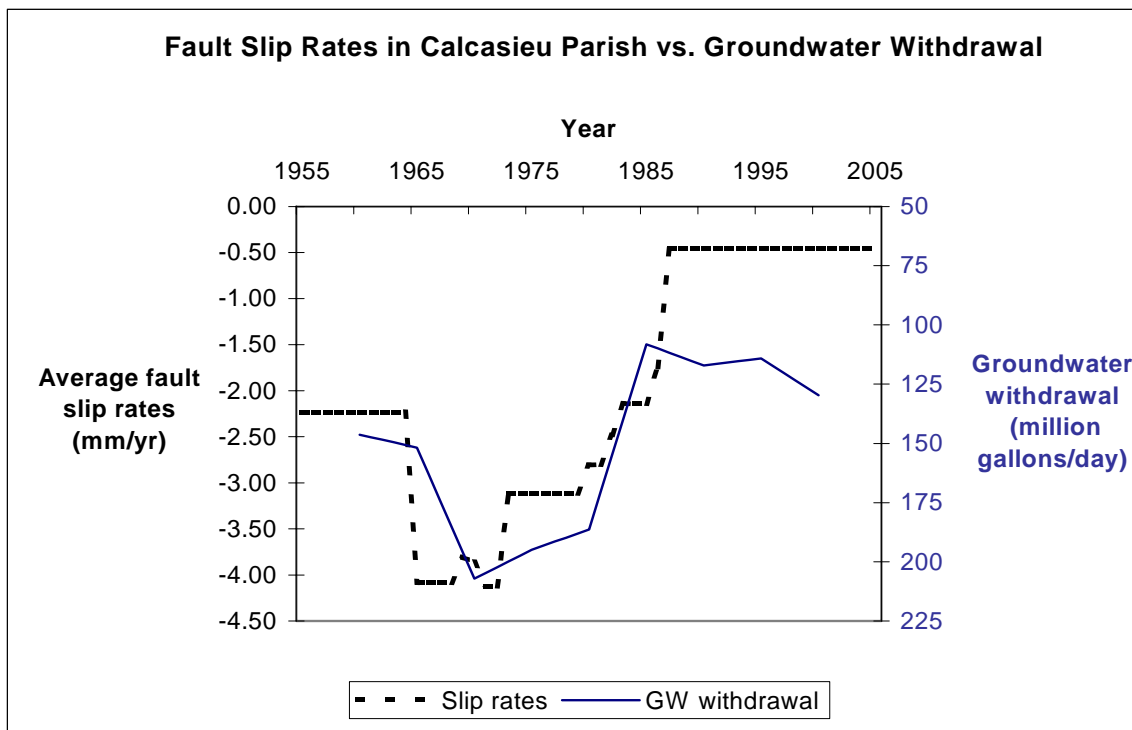


Figure 5.1. Graph of average slip rates vs. groundwater withdrawal in Calcasieu Parish over the past half-century.

5.3 Subsurface Fluid Withdrawal

The extraction of subsurface fluids (oil, gas, or water) results in decreases in fluid pressure in the reservoir and an increase in effective (grain to grain) stress (Holzer, 1984). This

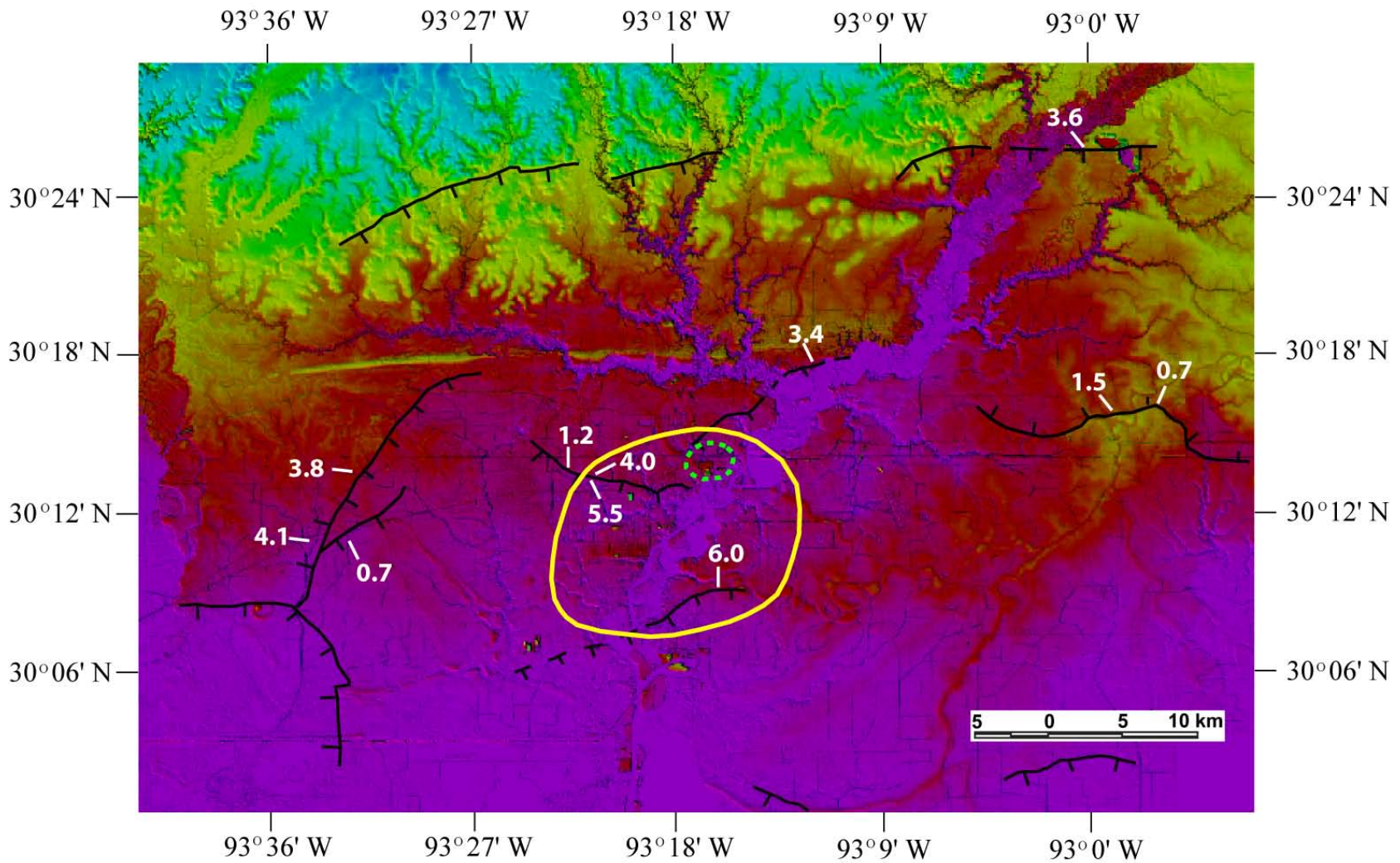


Figure 5.2. Spatial association of groundwater withdrawal with accelerated faulting. Black lines represent fault-related steps in the study area (teeth on downthrown side). Yellow circle contains area of greatest piezometric decline near the Lake Charles Industrial District. Green dashed circle marks the area of greatest measured subsidence. Numbers are vertical slip rates on faults during the late 1960's and early 1970's.

occurs because as fluid pressure declines, the pore fluid supports less of the weight of the overburden and this places more of the earth's stresses on the rock layers. If the pressure depletion is substantial, compaction of the reservoir or surrounding sediments may occur and translate to the surface as ground subsidence. In shallow unconsolidated sand bodies, such as groundwater aquifers, pore pressure reductions create relatively minor, elastic compaction of sediments. However, as water levels drop in the aquifer, pore fluids drain from the surrounding fine-grained confining layers (usually clay), causing a much greater amount of primarily inelastic compaction and subsequent subsidence. Estimates of subsidence due to groundwater withdrawal in the Gulf Coast range from around 1 ft in Baton Rouge to as much as 3 to 5 ft in the Houston-Galveston area (Poland, 1972). Several workers (Reid, 1973; Kreitler, 1976; Holzer, 1984) have suggested that differential subsidence across faults in the Houston area has accelerated fault creep in areas of subsurface fluid withdrawal. Because subsidence due to petroleum production is expected to be minor (Geertsma, 1973; Martin and Serdengecti, 1984; Holzer and Bluntzer, 1978), withdrawal of oil and gas is not considered here as a major contributor to historical faulting, at least not by a differential compaction mechanism. Since groundwater aquifers are relatively shallow, consist of unconsolidated sediment, and experience continuous withdrawals from relatively large areas, groundwater withdrawal is expected to be the primary cause for man-induced subsidence and faulting. Although no cause-and-effect relationship has been established for man-induced faulting, several studies have noted a spatial and temporal association between groundwater withdrawal and accelerated fault rates. Holzer and Gabrysch (1978) found that fault creep has stopped or slowed in the eastern area of Houston where reductions in groundwater pumping have allowed water levels to recover partially. They also concluded that the continued slow creep at an average rate of about 1 mm/yr in areas of water level recovery suggests that the historical faulting in the Houston area may not be completely related to groundwater withdrawal. The observations and conclusions Holzer and Gabrysch (1978) documented bear a striking resemblance to those presented here.

The study area and the Houston-Galveston area share similar aquifer conditions since most groundwater used in these localities is withdrawn from the Pleistocene Chicot Aquifer. The Chicot Aquifer system is the principle source for groundwater in southwestern Louisiana and is the most heavily pumped aquifer in the state (Nyman, 1990). In the Lake Charles area, water level reductions have been greater than in the outlying areas of southwestern Louisiana due to a large and continuous withdrawal from closely spaced wells (Harder et al., 1967). A large cone of depression, centered beneath Westlake in the Lake Charles Industrial District, is the result of intense groundwater pumping since the 1930's (Lovelace, 1998). This piezometric depression directly corresponds with an area of local subsidence near Westlake detected by analysis of geodetic data (Trahan, 1982; Jurkowski et al., 1984). Trahan (Figure 5.3) estimated that over 200 mm of subsidence had occurred in that locality between 1918 and 1972, however, this is a considerable underestimation, since the benchmark he used as a reference was also subsiding (Shinkle and Dokka, 2004) due to local and regional factors. According to the leveling lines that traverse through this local subsidence trough, the rates of negative vertical motion apparently reached a peak in the late 1960's and early 1970's and experienced a sharp decline after that (Appendix B). This corresponds well with a significant reduction in groundwater withdrawal and a subsequent rebound in piezometric levels in the Lake Charles area during that time. Lovelace (1998) reported that reliance on groundwater sources was reduced with the construction of the Sabine River Diversion Canal causing a sharp rise in water levels in the late 1970's and early 1980's. A record of water levels in Well Cu-77, near the area of maximum subsidence, shows a similar trend (Figure 5.4). Nearly all well records around the Lake Charles area show a stabilization of water levels in the early 1980's with very little change occurring in recent times. This trend is temporally associated with reductions in subsidence and faulting determined from leveling data, which indicates these processes could possibly be related.

While it appears that subsidence and accelerated faulting both result from subsurface fluid withdrawal, the mechanism by which they occur may differ. Holzer (1984) and Kreitler (1976)

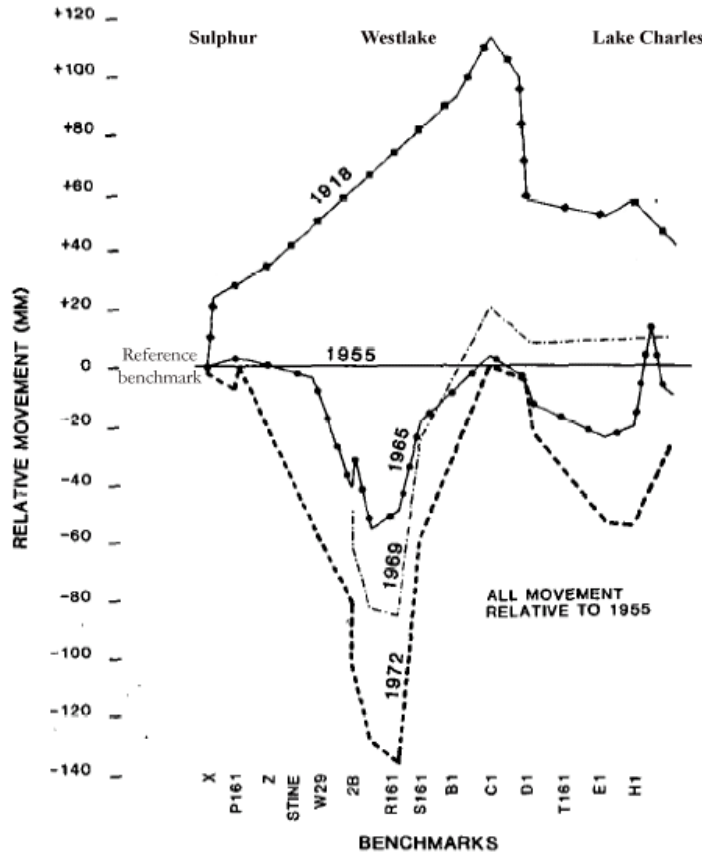


Figure 5.3. Subsidence of benchmarks in the Lake Charles Industrial District (modified from Trahan, 1982).

have argued that differential compaction across faults in the Gulf Coast accelerates fault displacement. If this were the case, faults should be downthrown toward the area of maximum groundwater withdrawal and subsidence. However, this relationship does not appear to exist in the study area, which suggests differential compaction is not the mechanism inducing fault motion here. The Sulphur and Moss Lake fault-related steps have both recently exhibited down-to-the-south displacement, opposite to the motion that would be expected if differential compaction were at work. The locations, orientations, and displacements of faults identified in this thesis indicate that the mechanism for human-accelerated faulting proposed by O'Neill and Van Siclen (1984) is more applicable for this locality. They inferred that a general lowering of the piezometric level is sufficient to accelerate the natural motion of pre-existing faults by

creating changes in the vertical effective stress. This process would be expected to result in increased slip rates along faults in areas where excessive groundwater withdrawal has created a depression in the piezometric surface. Because this process is independent of differential compaction, faults would not be downthrown towards areas of greater groundwater withdrawal, but rather would exhibit increased slip rates in the same manner the fault has exhibited throughout its history.

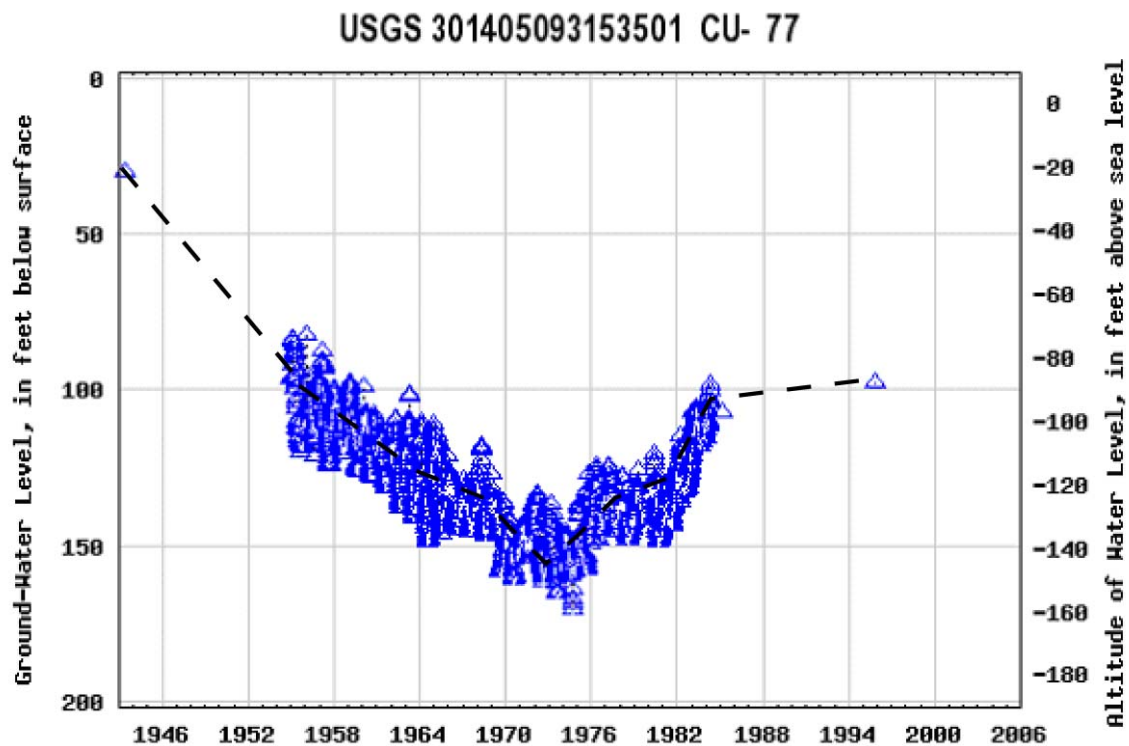


Figure 5.4. Record of water levels in well Cu-77 near Westlake in the Lake Charles Industrial District. (<http://la.water.usgs.gov>)

5.4 Neotectonic Structural Framework

Murray (1961) has identified several well-defined belts or zones of faults that extend east to west across the Gulf Coast Region (Figure 2.5). Subsurface data reveal that some are regional systems of down-to-the-south faults, while others are principally in the form of faults associated with salt structures. The subsurface evaluation presented in this paper has shown that several of the faults associated with these zones extend up to the land surface and are currently disrupting it.

Figure 5.5 ties this well-known structural framework of the subsurface with the newly mapped fault-related steps in the study area. The Tepehate-Baton Rouge System constitutes a fairly continuous *en echelon* zone of faults from the northern portion of study area eastward to Baton Rouge and eventually north of New Orleans. These faults are mostly major down-to-the-south growth faults associated with abnormal thickening of Jacksonian (Late Eocene) and Vicksburgian (Early Oligocene) strata. South of this zone is what Murray terms the Iowa fault system and Ocamb (1961) calls the Oligocene domal trend, where the majority of faults are related to salt movement. This relationship is evidenced by the spatial association of fault-related steps mapped by the author with the location of salt domes in the central portion of the study area. Concurrent with, and possibly preceding Oligocene deposition, upward movement of salt in this zone resulted in mostly radial and graben type faulting (Ocamb, 1961). The Moss Lake fault-related step shown in Figure 4.6 is part of Murray's Lake Arthur fault system, which can be traced from northwestern Cameron Parish, across Calcasieu and Jefferson Davis parishes and eventually intersects the Tepehate-Baton Rouge system to the east. The faults in this system are part of a larger regional growth fault trend associated with increases in Frio (Middle Oligocene) age strata. Just south of this zone lies Murray's Scott fault system, a zone of imperfectly known growth faulting associated with expansion of Anahuac (Late Oligocene) sediments (Murray, 1961). The obvious connection between this subsurface structural framework and the fault-related steps investigated in this study demonstrates that these features are indeed of tectonic origin and were not initially formed by human processes.

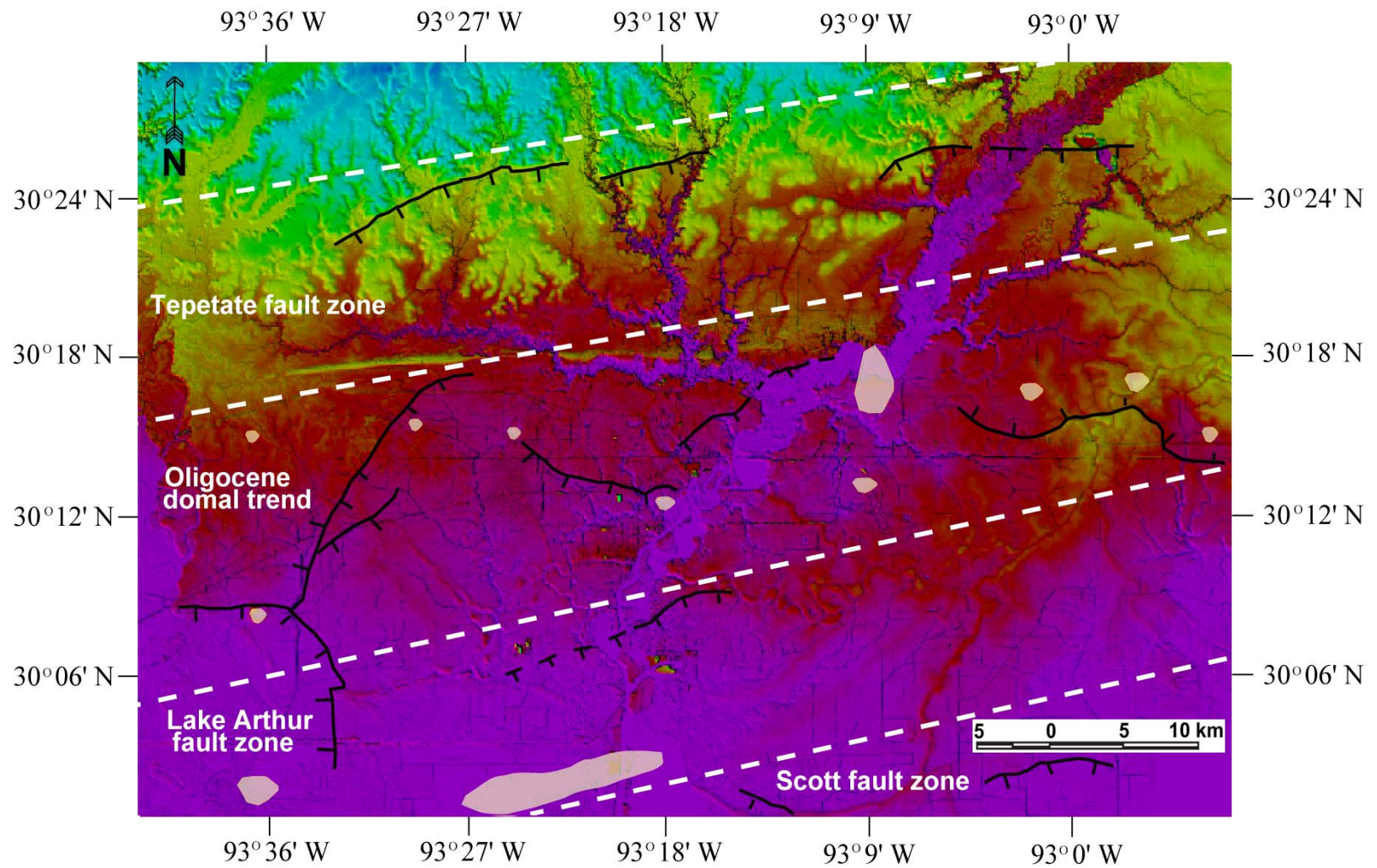


Figure 5.5. Neotectonic structural framework of the study area.

CHAPTER 6

CONCLUSIONS AND RECOMMENDATIONS

6.1 Conclusions

Due to the destruction of benchmarks, the short time range studied, and the lack of previous studies of fault activity in southwestern Louisiana, any conclusions about the causes for neotectonic activity in this area are somewhat speculative. However, the analysis presented herein, when reviewed in the context of other cases of Gulf Coast neotectonics, provides a better understanding of not only the nature of fault motion in the study area, but also the causes of this active faulting. This preliminary investigation of neotectonics in the study area indicates that recent fault motions may be decelerating due to reductions in subsurface fluid withdrawal, although unequivocal proof is lacking. The possibility of a regional reduction in the natural episodic slip rates of these faults cannot be discounted. From these results, the following conclusions can be drawn:

1. Several linear to arcuate geomorphic features have been identified in southwestern Louisiana and appear to represent the surface expressions of known subsurface faults.
2. These faults are currently active and have caused deformation of the ground surface and disrupted built structures located near them.
3. Geodetic evidence has revealed that most of these faults experienced reduced rates of motion since the 1960's and 1970's when displacements were several times greater.
4. Natural geologic forces, such as lithospheric flexure and salt movement, undoubtedly play some role in the formation and current activity of these faults. However, because modern rates of fault motion are far in excess of geologic slip rates, other factors are likely at work.
5. The close spatial and temporal association of increased subsurface fluid withdrawal with fault acceleration suggests these processes may be related.
6. Lowering of the piezometric surface in the study area appears to have created changes in the effective stress field, thereby increasing the natural motion on these faults.

7. Although human-induced faulting seems likely, the episodic nature of these faults does not rule out the possibility of periods of geologically high slip rates.

6.2 Recommendations

Based on the findings of this thesis, the following recommendations are made:

1. For improved kinematic evaluation, a denser network of benchmarks should be established on both sides of these fault-related steps. A similar array of control points has been placed near faults in the Houston area to improve investigations there and could prove useful in the study area.
2. The leveling technique used in this study should be performed in the future to continually determine the nature of faulting in southwest Louisiana.
3. The ongoing motion of these faults should be taken into consideration when planning any construction or engineering works near the fault-related steps identified in this study.
4. Detailed subsurface investigations, incorporating soil boring logs, high-resolution seismic surveys and shallow resistivity data, should be performed near these fault-related steps to locate their associated fault planes and confirm their correlation with known subsurface faults.

REFERENCES

- Anderson, J.M., and E.M. Mikhail, 1998. *Surveying; Theory and Practice*, 7th ed., McGraw-Hill, New York, 1167 pp.
- Atwater, G.I., and M.J Forman, 1959. Nature of growth of southern Louisiana salt domes and its effect on petroleum accumulation: *Bulletin, American Association of Petroleum Geologists*, v. 43, no. 11, pp. 2592-2622.
- Bebout, D.G., and D.R. Gutiérrez, 1983. *Regional cross sections, Louisiana Gulf Coast. Louisiana Geological Survey Folio Series 6*, Baton Rouge, LA.
- Bellamy, J., 1970. Topsy-Thompson Bluff-Indian Village fields, Jefferson Davis Parish, Louisiana: *Typical oil and gas fields of southwestern Louisiana*, v. 2, pp. 28-28b.
- Benson, P. H., 1971. Geology of the Oligocene Hackberry trend, Gillis English bayou-Manchester area, Calcasieu parish, Louisiana: *Transactions, Gulf Coast Association of Geological Societies*, v. 21, pp. 1-14.
- Bossler, J.D., 1984. *Standards and specifications for geodetic surveys. National Geodetic Survey, Rockville, MD*, 29 pp.
- Bruce, C.M., 1973. Pressured shale and related sediment deformation: mechanism for development of regional contemporaneous faults: *Bulletin, The American Association of Petroleum Geologists*, v. 57, no. 5, pp. 878-886.
- Brunhild, S.R., 1984. Depositional and structural reconstruction of southwestern Louisiana Oligo-Miocene strata; a temporal-spatial approach: *Transactions, Gulf Coast Association of Geological Societies*, v. 34, pp. 9-31.
- Cartwright, J., R. Bouroullec, D. James, and H. Johnson, 1998. Polycyclic motion history of some Gulf Coast growth faults from high-resolution displacement analysis: *Geology*, v.26, no.9, pp. 819-822.
- Cazes, C.A., 2004. *Overlap Zones, Growth Faults, and Sedimentation: Using High Resolution Gravity Data, Livingston Parish, Louisiana. Louisiana State University, Master's thesis.*
- Clanton, U. S., and E. R. Verbeek, 1979. Faults offsetting land surfaces in southeastern Houston metropolitan area, Texas: *Bulletin, American Association of Petroleum Geologists*, v. 63, no. 3, pp. 432.
- Cloos, E., 1968. Experimental analysis of Gulf Coast fracture patterns: *Bulletin, American Association of Petroleum Geologists*, v. 52, no. 3, pp. 420-444.
- Codina, J., 1964. East Moss Lake Field, Calcasieu Parish, Louisiana: *Typical oil and gas fields of southwestern Louisiana*, pp. 8-8b.
- Cossey, S. J., and R. E. Jacobs, 1992. Oligocene Hackberry Formation of Southwest Louisiana; sequence stratigraphy, sedimentology, and hydrocarbon potential: *Bulletin, American Association of Petroleum Geologists*, v. 76, no. 5, pp. 589-606

Crans, W., G. Mandl, and J. Haremboure, 1980. On the theory of growth faulting: a geomechanical model based on gravity sliding: *Journal of Petroleum Geology*, v.2, no.3, pp. 265-307.

Diegel, F. A., J. F. Karlo, D. C. Schuster, R. C. Shoup, and P.R. Tauvers, 1995. Cenozoic structural evolution and tectonostratigraphic framework of the northern Gulf Coast continental margin, *in* M. P. A. Jackson, D. G. Roberts, and S. Snelson, eds., *Salt tectonics: a global perspective*: AAPG Memoir 65, pp. 109–151.

Dokka, R.K., 2004. Structural characteristics of active normal faults in south Louisiana; implications for their origin and public policy: *Abstracts with Programs, Geological Society of America*, v. 36, no. 1, pp. 26.

Dula, W.F., Jr., 1991. Geometric models of listric normal faults and rollover folds: *Bulletin, American Association of Petroleum Geologists*, v. 75, no. 10, pp. 1609-1625.

Durham, C.O., Jr. and E.M. Peebles, III, 1956. Pleistocene fault zone in southeastern Louisiana: *Transactions, Gulf Coast Association of Geological Societies*, v.5, pp. 65.

Eby, J.B., 1943. Geophysical history of the Iowa field, Calcasieu and Jefferson Davis Parishes, Louisiana: *Geophysics*, v. 8, no. 4, pp. 348-355.

Edwards, M.B., 1991. Control of depositional environments, eustacy, and gravity and salt tectonics on sandstone distribution in an unstable shelf edge delta, Eocene Yegua Formation, Texas and Louisiana: *Transactions, Gulf Coast Association of Geological Societies*, v. 41, pp. 237-252.

Ewing, T.E., 1991. Structural framework *in* Salvador, A., ed. *The Gulf of Mexico Basin*: Boulder, Colorado, Geological Society of America, *The Geology of North America*, v. J.

Ewing, T.E., 1983. Growth faults and salt tectonics in Houston diapir province; relative timing and exploration significance: *Transactions, Gulf Coast Association of Geological Societies*, v. 33, pp. 83-90.

Fails, T.G., 1990. Variation in salt dome faulting, Coastal Salt Basin: *Transactions, Gulf Coast Association of Geological Societies*, v. 40, pp. 181-193.

Fendick, R.B., and D.J. Nyman, 1987. Louisiana ground-water map No. 1; potentiometric surface, 1985, and water-level changes, 1983-85, of the Chicot Aquifer in southwestern Louisiana. *Water-Resources Investigations*, U. S. Geological Survey, Reston, VA.

Feng, J., and R.T. Buffler, 1996. Post Mid-Cretaceous depositional history, Gulf of Mexico: *Bulletin, American Association of Petroleum Geologists*, v. 80, no. 9, pp. 1501.

Friedel, G. F., 1978. Structural and geothermal relationships in the Lake Charles area of southwestern Louisiana. University of Southwestern Louisiana, Master's thesis.

Gagliano, S. M., E.B. Kemp, K.M. Wicker, K.S. Wiltenmuth, and R. Sabate, 2003. Neo-tectonic framework of southeast Louisiana and applications to coastal restoration: *Transactions, Gulf Coast Association of Geological Societies*, v. 53, pp. 262-276.

Galloway, W.E. 1986. Growth faults and fault-related structures of prograding terrigenous clastic continental margins: Transactions, Gulf Coast Association of Geological Societies, v. 36, pp. 121-128.

Geertsma, J., 1973. Land subsidence above compacting oil and gas reservoirs: Journal of Petroleum Technology, v. 25, no. 6, pp. 734-744.

Hanor, J.S., 1982. Reactivation of fault movement, Tepeate fault zone, south central Louisiana: Transactions, Gulf Coast Association of Geological Societies, v. 32, pp. 237-245.

Harder, A.H., 1960. The geology and ground-water resources of Calcasieu Parish, Louisiana. U.S. Geological Survey, Reston, VA, 102 pp.

Harder, A. H., C. Kilburn, H. M. Whitman, and S. M. Rogers, 1967. Effects of ground-water withdrawals on water levels and salt-water encroachment in southwestern Louisiana. Louisiana Geol. Survey and Dept. Public Works Water Resources Bulletin, v. 10, 56 pp.

Hardin, F.R., and C. Hardin, Jr., 1961. Contemporaneous normal faults of Gulf Coast and their relation to flexures: Bulletin, American Association of Petroleum Geologists, v. 45, no. 2, pp. 238-248.

Heinrich, P.V., 2000. DeQuincy Fault-Line Scarp, Beauregard and Calcasieu Parishes, Louisiana: Basin Research Institute Bulletin, v. 9, pp. 38-50.

Heinrich, P.V., 1988. Tectonic origin of Montgomery Terrace scarp of southwestern Louisiana: Bulletin, American Association of Petroleum Geologists, v. 72, no. 9, pp. 1113.

Heinrich, P.V., 1997. Pleistocene fault-line scarps and neotectonics in Southwest Louisiana: Abstracts with Programs, Geological Society of America, v. 29, no. 3, pp. 23.

Hickey, M., and R. Sabate, 1972. Tectonic map of Gulf coast region, U.S.A. Gulf Coast Association of Geological Societies and American Association of Petroleum Geologists, Tulsa, OK.

Holdahl, S.R., 1976. Comment on "New Vertical Geodesy" by J.H. Whitcomb: Journal of Geophysical Research, v. 81, no. 26, pp. 4945-4946.

Holdahl, S.R., and N.L. Morrison, 1974. Regional investigations of vertical crustal movements in the U.S., using precise relevelings and mareograph data: Tectonophysics, v. 23, no. 4, pp. 373-390.

Holzer, T.L., 1984. Ground failure induced by ground-water withdrawal from unconsolidated sediment: Reviews in Engineering Geology, v. 6, pp. 67-105.

Holzer, T.L., and R.L. Bluntzer, 1984. Land subsidence near oil and gas fields, Houston, Texas: Ground Water, v. 22, no. 4, pp. 450-459.

Holzer, T. L., and R.K. Gabrysch, 1987. Effect of water-level recoveries on fault creep, Houston, Texas: Ground Water, v. 25, no. 4, pp. 392-397.

<http://la.water.usgs.gov> USGS website with well records for the state of Louisiana

<http://www.ngs.noaa.gov/datasheet.html> NGS website for publishing benchmark information.

Humphris, C. C., Jr., 1979. Salt movement on continental slope, northern Gulf of Mexico: Bulletin, American Association of Petroleum Geologists, v. 63, no. 5, pp. 782-798.

Ingram, R.J., 1991. Salt Tectonics: An Introduction to Central Gulf Coast Geology, pp 31-60.

Jurkowski, G., J. Ni, and L. Brown, 1984. Modern uparching of the Gulf coastal plain: Journal of Geophysical Research, v.89, pp. 6247-6262.

Kearby, J. K., 1989. DeQuincy-East Perkins Field; Calcasieu Parish, Louisiana: Typical oil and gas fields of southwestern Louisiana, pp. 6-6c.

Kebede, A.E., 2002. Movement Along the Baton Rouge Fault, Louisiana. Louisiana State University, Master's thesis.

Kreitler, C. W., 1976. Active surface faulting, Texas coastal zone: Bulletin, American Association of Petroleum Geologists, v. 60, no. 4, pp. 689

McCulloh, R., 2001. Active Faults in East Baton Rouge Parish. Louisiana Geological Survey, Public Information Series No. 8, Baton Rouge, La., 5 pp.

LeVie, D., 1985. Interdomal sediment ponding; a new Lower Hackberry play?: Transactions, Gulf Coast Association of Geological Societies, v. 35, pp. 171-178.

Lopez, J. A., S. Penland, and S. J. Williams, 1997. Confirmation of active geologic faults in Lake Ponchartrain in Southeast Louisiana: Transactions, Gulf Coast Association of Geological Societies, v. 47, pp. 299-303.

Lovelace, J.K., 1998. Distribution of saltwater in the Chicot Aquifer system in the Calcasieu Parish area, Louisiana, 1995-96. Water Resources Technical Report, no. 62, Baton Rouge, La., 59 pp.

Lovelace, J.K., J.W. Fontenot, and C.P. Frederick, 2002. Potentiometric surface of the Chicot aquifer system in southwestern Louisiana, January 2001. Water-Resources Investigations, U. S. Geological Survey, Reston, VA.

Martin, J. C., and S. Serdengecti, 1984. Subsidence over oil and gas fields: Reviews in Engineering Geology, v. 6, pp. 23-34.

McCulloh, R.P., and W. J. Autin, 1991. Revised mapping of subsurface faults, East Baton Rouge Parish, Louisiana: Bulletin, American Association of Petroleum Geologists, v.75, no. 9, pp. 1533.

Miller, B., and P.V. Heinrich, 2003. Hydrocarbon production and surface expression of the China Segment of the Tepehate fault zone, Louisiana: Transactions, Gulf Coast Association of Geological Societies, v. 53, pp. 548-554.

Morton, R.A., N.A. Purcell, and R.L. Peterson, 2001. Field evidence of subsidence and faulting induced by hydrocarbon production in coastal Southeast Texas: Transactions, Gulf Coast Association of Geological Societies, 2001, v. 51, pp. 239-248.

- Murray, G.E., 1961. Geology of the Atlantic and Gulf coastal province of North America. New York, Harper Brothers, 692 pp.
- Nelson, T.H., 1991. Salt tectonics and listric-normal faulting, *in* Salvador, A., ed., The Gulf of Mexico Basin: Boulder, Colorado, Geological Society of America, The Geology of North America, v. J.
- Nicol, A., J. J. Walsh, J. Watterson, and J. R. Underhill, 1997. Displacement rates of normal faults: *Nature*, v. 390, no. 6656, pp. 157-159.
- Nunn, J.A., 2003. Land surface subsidence caused by groundwater withdrawal in southeastern Louisiana: *Transactions, Gulf Coast Association of Geological Societies*, v. 53, pp. 630-638.
- Nunn, J.A., 1985. State of stress in the northern Gulf Coast: *Geology*, v. 13, pp. 429-432.
- Nyman, D.J., 1984. The occurrence of high concentrations of chloride in the Chicot aquifer system of southwestern Louisiana. *Water Resources Technical Report, Baton Rouge, La.*, v. 33, 75 pp.
- Nyman, D. J., K.J. Halford, and A. Martin, 1990. Geohydrology and simulation of flow in the Chicot Aquifer system of southwestern Louisiana. *Water Resources Technical Report, Baton Rouge, La.*, 58 pp.
- Ocamb, R.D., 1961. Growth faults of south Louisiana: *Transactions, Gulf Coast Association of Geological Societies*, v. 11, pp. 139-175.
- O'Neill, M.W., and D.C. Van Siclen, 1984. Activation of Gulf Coast faults by depressuring of aquifers and an engineering approach to siting structures along their traces: *Bulletin of the Association of Engineering Geologists*, v. 21, no. 1, pp. 73-87.
- Paine, W. R., 1968. Stratigraphy and sedimentation of subsurface Hackberry wedge and associated beds of southwestern Louisiana: *Bulletin, American Association of Petroleum Geologists*, v. 52, no. 2, pp. 322-342.
- Paine, W. R., 1962. Geology of Acadia and Jefferson Davis Parishes. *Louisiana Geological Survey Bulletin, Baton Rouge, LA*, 277 pp.
- Parker, S.P., 1984. *McGraw-Hill Dictionary of Earth Sciences*. McGraw-Hill Book Company, New York, 837 pp.
- Peel, F. J., C. J. Travis, and J. R. Hossack, 1995. Genetic structural provinces and salt tectonics of the Cenozoic offshore U.S. Gulf of Mexico; a preliminary analysis, *in* M. P. A. Jackson, D. G. Roberts, and S. Snelson, eds., *Salt tectonics: a global perspective: Memoir, American Association of Petroleum Geologists*, v. 65, pp. 153-175.
- Poland, J. F., 1972. Subsidence and Its Control: *Memoir, American Association of Petroleum Geologists*, v. 18, pp. 50-71.
- Pyle, G. T., and J. Babisak, 1951. The structure of Woodlawn Field, Jefferson Davis Parish, Louisiana: *Transactions, Gulf Coast Association of Geological Societies*, v. 1, pp. 200-210.

- Rainwater, E. H., 1964. Regional Stratigraphy of the Gulf Coast Miocene: Transactions, Gulf Coast Association of Geological Societies, v. 14, pp. 81-124.
- Reid, W. M., 1973. Active faults in Houston, Texas: Abstracts with Programs, Geological Society of America, v. 5, no. 7, pp. 777-778.
- Salvador, A., 1991. Origin and development of the Gulf of Mexico basin, *in* Salvador, A., ed. The Gulf of Mexico Basin: Boulder, Colorado, Geological Society of America, The Geology of North America, v. J.
- Scholz, C.H., 1998. Earthquakes and friction laws: Nature, v. 391. no. 6662, pp. 37-42.
- Schomaker, C.M., and R.M. Berry, 1981. NOAA Manual NOS NGS 3, 1981. National Geodetic Survey, Rockville Md.
- Schultz, J.R., and A.B. Cleaves, 1955. Geology in Engineering. Wiley, New York, 592 pp.
- Shelton, J.W., 1984. Listric normal faults: an illustrated summary: Bulletin, American Association of Petroleum Geologists, v. 68, no. 7, pp. 801-815.
- Shinkle, K. and R. K. Dokka, 2004. Rates of vertical displacement at benchmarks in the lower Mississippi Valley and the northern Gulf Coast. NOAA Technical Report 50, National Geodetic Survey, Rockville, Md., 135 pp.
- Smith, C.G., and C.G. Kazmann, 1978. Subsidence in the Capital Area Ground Water Conservation District – an update: Capital Area Ground Water Conservation Commission Bulletin, no. 2, 31 pp.
- Snead, J.I., P.V. Heinrich, and R.P. McCulloh, 2002. Lake Charles 30 x 60-minute geologic quadrangle. Louisiana Geological Survey, Baton Rouge, La.
- Spencer, J. A., and C. L. Sharpe, 1996. Evolution of salt and hydrocarbon migration; Sweet Lake area, Cameron Parish, Louisiana: Transactions, Gulf Coast Association of Geological Societies, v. 46, pp. 383-390.
- Spencer, J. A. and C. L. Sharpe, 1993. Deep-seated salt sheet; eastern Calcasieu Parish, Louisiana: Transactions, Gulf Coast Association of Geological Societies, v. 43, pp.363-371.
- Tabbi-Annani, A., 1975. Subsurface geology of south-central Calcasieu Parish, Louisiana. University of Southwestern Louisiana, Master's thesis.
- Thorsen, C., 1963. Age of growth faulting in southeast Louisiana: Transactions, Gulf Coast Association of Geological Societies, v. 13, pp. 103-110.
- Trahan, D.B., 1982. Monitoring local subsidence in areas of potential geopressed fluid withdrawal, southwestern Louisiana: Transactions, Gulf Coast Association of Geological Societies, v. 32, pp. 231-236.
- Troutman, A., 1955. The oil and gas fields of Southwest Louisiana, xiii. Five Star Oil Report, Houston, Texas, 376 pp.

- Van Siclen, D.C., 1972. Reply; The Houston Fault Problem: Bulletin of the Association of Engineering Geologists, v. 9, no. 1, pp. 69-77.
- Verbeek, E. R., 1979. Quaternary fault activity in Texas Gulf Coast: Bulletin, American Association of Petroleum Geologists, v. 63, no. 3, pp. 545.
- Verbeek, E. R., K.W. Ratzlaff, and U.S. Clanton, 1979. Faults in parts of north-central and western Houston metropolitan area. Texas Miscellaneous Field Studies Map, U. S. Geological Survey, Reston, VA.
- Visser, W.A., 1980. Geological Nomenclature. Royal Geological and Mining Society of the Netherlands, The Hague, 540 pp.
- Walcott, R. I., 1972. Gravity, Flexure, and the Growth of Sedimentary basins at a Continental Edge: Geological Society of America Bulletin, v. 83, no. 6, pp. 1845-1848.
- Wallace, W. E., 1966. Fault and salt map of South Louisiana: Transactions, Gulf Coast Association of Geological Societies, v. 16, pp. 373.
- Walters, D.J., 1996. Louisiana ground-water map no. 10; potentiometric surface, 1991, and water-level changes, 1985-91, of the Chicot aquifer system in southwestern Louisiana. Water-Resources Investigations, U. S. Geological Survey, Reston, VA.
- White, W.A., and R.A. Morton, 1997. Wetland losses related to fault movement and hydrocarbon production, southeastern Texas coast: Journal of Coastal Research, v. 13, no. 4, pp. 1305-1320.
- White, W.A., and T.A. Tremblay, 1995. Submergence of wetlands as a result of human-induced subsidence and faulting along the upper Texas Gulf Coast: Journal of Coastal Research, v. 11, no. 3, pp. 788-807.
- Wilson, F., and J.A. Noel, 1983. Gravity analysis of west-central Calcasieu Parish, Louisiana: Transactions, Gulf Coast Association of Geological Societies, v. 33, pp.243-250.
- Winker, C.D., 1983. Unstable progradational clastic shelf margins: Special Publication, Society of Economic Paleontologists and Mineralogists, v. 33, pp. 139-157.
- Winker, C.D., 1982. Cenozoic shelf margins, northwestern Gulf of Mexico: Transactions, Gulf Coast Association of Geological Societies, v. 32, pp. 427-448.
- Wintz, W.A. Jr., R.G. Kazmann, and C.G. Smith, 1970. Subsidence and ground-water offtake in the Baton Rouge Area. Louisiana State University, Louisiana Water Resources Research Institute, Bulletin, no. 6, 20 pp.
- Worrall, D.M., and S. Snelson, 1989. Evolution of the northern Gulf of Mexico, *in* Bally, A.W., and Palmer A.R., eds., The Geology of North America—An overview, Boulder, Colorado, Geological Society of America, Geology of North America, v. A, pp. 97-138.
- Yerkes, R. F., and R. O. Castle, 1976. Seismicity and faulting attributable to fluid extraction: Engineering Geology, v. 10, pp. 151-167.

APPENDIX A GLOSSARY

allochthonous: a rock mass that has been displaced over a considerable distance.

antithetic fault: auxiliary fault whose sense of displacement is opposite to the major fault.

aseismic creep: fault movement that does not generate earthquakes.

autochthonous: a rock mass that is found more or less in the place where it was formed.

cataclastic flow: a type of rock deformation that occurs by fracture and rotation of aggregates or mineral grains.

decollement: the sliding of one rock mass over another one.

diapirism: the piercement of relatively light and mobile rock material through or into an overlying sequence.

downwarping: A broad downward bending of a segment of the earth's crust.

effective stress: the stress transmitted from particle to particle in a soil or rock mass. In water saturated soil and rock, the effective stress is the difference between the total stress and the pore pressure.

en echelon: referring to the overlapped or staggered arrangement of geologic features.

fault: a fracture along which adjacent rock surfaces are differentially displaced.

fault trace: intersection of the fault plane with the surface of the earth or any horizontal surface.

fault-line scarp: a relatively steep escarpment that is the result of differential erosion along a fault trace rather than the direct result of fault motion.

footwall: the rock mass below a fault plane.

geomorphology: the description of natural phenomena and the investigation of the history of geologic changes through the interpretation of topographic forms.

graben: a block of the earth's crust that has dropped down relative to blocks on either side.

hanging wall: the rock mass above a fault plane.

neotectonics: the study of the most recent structures and structural history of the earth's crust.

net slip: the distance between two formerly adjacent points on either side of a fault; defines the direction and relative amount of vertical and horizontal displacement.

normal fault: a fault in which the hanging wall has moved down relative to the footwall.

piezometric level: the level to where water would rise in an observation well due to the pressure in a reservoir.

progradation: a seaward outbuilding that results from sediment accumulation or deposition.

reservoir pressure: the pressure prevailing in the fluids occupying the pore volume in the reservoir rock. Also known as pore pressure or fluid pressure.

reverse fault: a fault in which the footwall has moved down relative to the hanging wall.

vertical slip: the vertical component of the net slip of a fault.

APPENDIX B SUBSIDENCE PROFILE

Relative motion of benchmarks in Calcasieu Parish since 1955

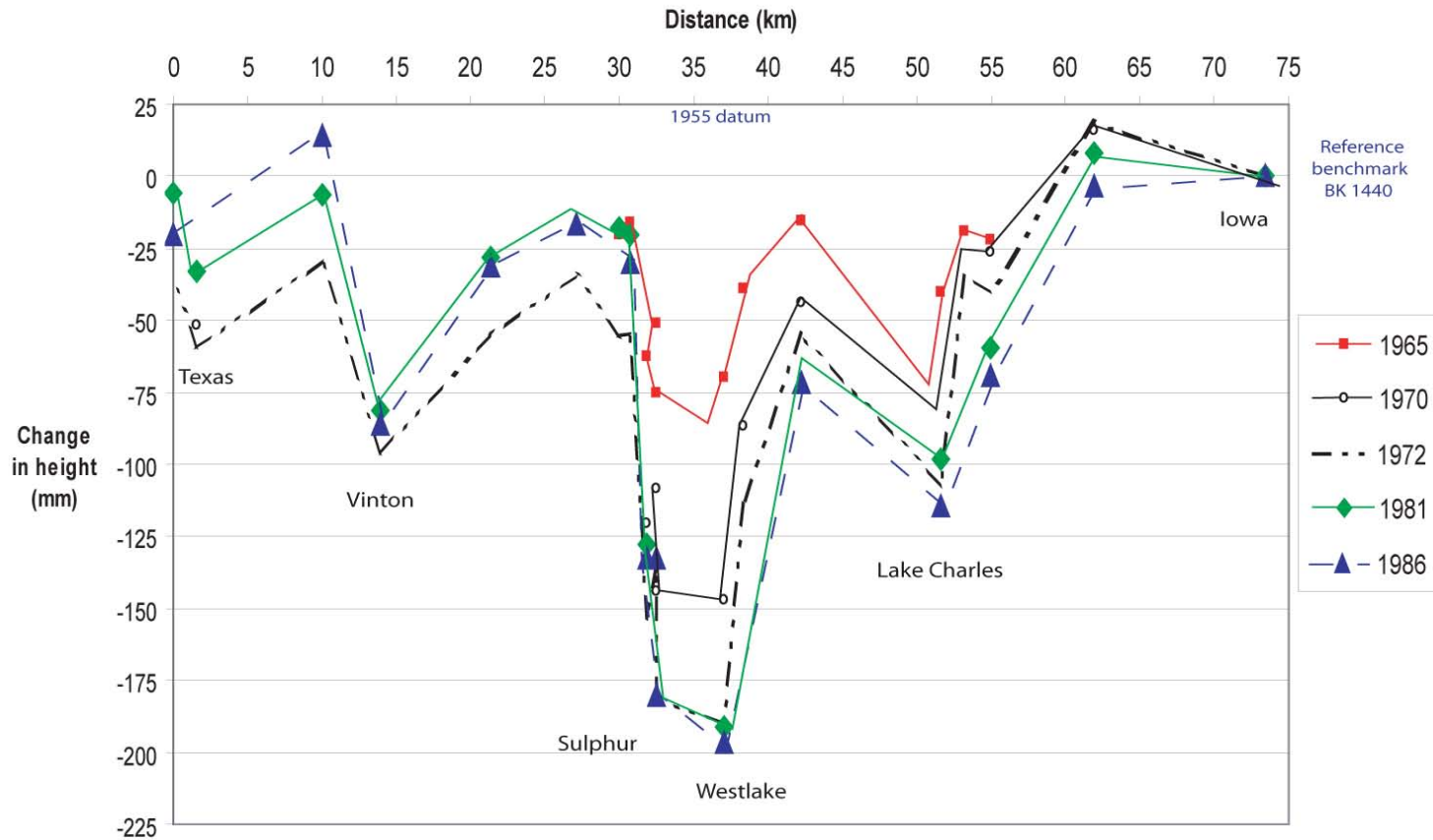


Figure B.1. Relative subsidence profile through the study area.

APPENDIX C FIELD PHOTOGRAPHS



Figure C.1. Photo of the Iowa fault-related step near Iowa. The dashed line represents the approximate location of the fault trace. Note that the north side of the fault is downthrown relative to the south side.



Figure C.2. Photo of the Moss Lake fault-related step near Moss Lake. The dashed line represents the approximate location of the fault trace.



Figure C.3. Photo of the Sulphur fault-related step near Sulphur. The dashed line represents the approximate location of the fault trace.



Figure C.4. Photo of the Sulphur fault-related step near Westlake. The dashed line represents the approximate location of the fault trace.



Figure C.5. Photo of the Moss Bluff fault-related step near Moss Bluff. The dashed line represents the approximate location of the fault trace.



Figure C.6. Photo of the DeQuincy fault-related step near Perkins. The dashed line represents the approximate location of the fault trace.

VITA

Jordan Oliver Heltz was born on December 5, 1978, to Michael and Libby Heltz, in Baton Rouge, Louisiana. He was raised in Lutcher, Louisiana, where he attended Lutcher High School until his graduation in 1996. After completing high school, Jordan attended Louisiana State University in Baton Rouge to pursue a Bachelor of Science degree in geology, which he received in December of 2000. He then entered the workforce for two years, attaining employment as a logging and directional drilling engineer in the oilfield.

In January of 2003, Jordan decided to return to LSU to pursue a Master of Science in Engineering Science degree. His graduate studies focused primarily on structural geology and civil engineering. After posting a 4.0 grade point average in his graduate work, Jordan plans to receive his master's degree in August 2005. During graduate school, he completed a geoscience internship with Unocal in Sugarland, Texas, and also received a full-time employment offer from the company. Upon graduation, Jordan plans to move to Houston, Texas, and work as an exploration geologist with Unocal.